The application of qPCR for characterization of LQTS-specific cardiomyocytes derived from induced pluripotent stem cells

Kiti Paavola

Master's Thesis

University of Tampere

Institute of Biosciences and Medical Technology (BioMediTech)

May 2015

Acknowledgements

This study was carried out in Heart Group, BioMediTech, University of Tampere. I am grateful to Heart Group leader, Professor Katriina Aalto-Setälä for allowing me to perform my Master's thesis studies in the Heart Group. I enjoyed working in that positive and innovative working environment occurred in the Heart Group. I want to say million thanks to my supervisor, Mari Pekkanen-Mattila for providing support and excellent advising during this work. I want to thank Anna Kiviaho for advising me in allelic imbalance determinations and allowing me to be one of the authors in the research article based on Anna's doctoral studies. Many thanks for Henna Venäläinen, Markus Haponen and Merja Lehtinen for technical assistance concerning cell culturing and plasmid preparations.

Special thanks I want to dedicate to my parents, Merja and Pertti, and siblings, Mari, Petra, Jere and Jesse, and their families, for all those supportive and encouraging words that I have got during this process. You have really helped me to accomplish this long-lasting process. I love you. Finally, the greatest thanks go to my fiancé Jonne who have being there for me in days full of tiredness and stress. That has meant a lot to me.

Tampere 8.5.2015

Kiti Paavola

Master's Thesis

Place: UNIVERSITY OF TAMPERE, Institute of Biosciences and Medical Technology (BioMediTech)
Author: PAAVOLA, KITI ANNA EMILIA

Title: The application of qPCR for characterization of LQTS-specific cardiomyocytes derived from induced pluripotent stem cells.

Pages: 70 pp.
Supervisor: Dr. Mari Pekkanen-Mattila, PhD
Reviewers: Professor Markku Kulomaa and Dr. Mari Pekkanen-Mattila, PhD
Date: May 2015

Abstract

Background and aims: Long QT syndrome (LQTS) is an inherent cardiac disorder causing severe arrhythmias due to mutations in cardiac ion channel genes. Four founder mutations causing LQTS have been identified from Finland and they disrupt functions of cardiac potassium ion channels. The aim of this study was to characterize expressions of ion channel genes or their allelic expression variation in three different experiments by using qPCR. In cell line characterization experiment was evaluated applicability of cell lysis -based genotyping method to characterize cardiac cell lines. The aim of the second experiment was to evaluate impacts of allelic expression differences on disease phenotype variation and development. The last experiment was used for examining capacity of single-cell qPCR method to detect specific gene expression within single cardiomyocytes.
Methods: qPCR was used to detect mRNA levels of ion channel genes or structural genes within LQTS-specific cardiomyocytes. The TaqMan® Sample-to-SNP™ Kit was tested in order to characterize *KCNQ1* mutated heterozygous cardiac cell lines. Allelic imbalance determination was performed using plasmid-derived standard curve method for each Finnish founder mutations. The Single cell-to-CT™ Kit was used to detect expression of *TNNT2* at the single cell level and cell population level.
Results: The used cell lysis -based genotyping method succeeded to characterize cardiac cell lines and any disruption was not detected during analyses. Allelic imbalance determination study revealed that KCNQ1-FinA and KCNQ1-FinB specific cardiomyocytes expressed alleles of *KCNQ1* with allelic ratios 3:1 indicating that expression of wild type allele was three-fold as compared to expression of mutant allele within these LQT1-specific cells. The Single cell-to-CT™ Kit did not manage to detect gene expression of *TNNT2* within single cell samples and its expression at population level was also reduced.
Conclusions: The detected allelic ratio 3:1 (WT:MUT) within KCNQ1-FinA and KCNQ1-FinB mutated cardiomyocytes could result in milder phenotypic effects due to that higher expression of wild type alleles may suppress effects of mutations. Milder phenotypic effects have been thought to be reason for unique enrichment of founder mutations among Finnish population. Therefore, allelic imbalance occurring in disease-causing genes can be a significant disease phenotype modifier. To validate this hypothesis, larger study population of mutation carriers with high phenotypic variation is needed. If correlation between allelic imbalance and phenotypic variation is detected, the allelic expression variation might be confirmed to be one explaining genetic factor to affect phenotypic variation.

Pro Gradu -tutkielma

Paikka: TAMPEREEN YLIOPISTO, BioMediTech
Tekijä: PAAVOLA, KITI ANNA EMILIA
Otsikko: qPCR-menetelmän hyödyntäminen indusoiduista pluripotenteista kantasoluista erilaistettujen LQTS-spesifisten sydänlihassolujen karakterisoinnissa.
Sivumäärä: 70 s.
Ohjaaja: FT. Mari Pekkanen-Mattila
Tarkastajat: Professori Markku Kulomaa ja FT. Mari Pekkanen-Mattila
Päiväys: Toukokuu 2015

Tiivistelmä

Tutkimuksen tausta ja tavoitteet: Pitkä QT oireyhtymä on vakavia rytmihäiriöitä aiheuttava perinnöllinen sairaus, joka johtuu mutaatioista sydänlihassolun ionikanavageeneissä. Suomessa vallitsee neljä pitkä QT oireyhtymää aiheuttavaa perustajamutaatiota, jotka heikentävät sydänlihassolujen kalium-ionikanavien toimintaa. Tämän tutkimuksen tavoitteena oli karakterisoida LQTS-spesifisten sydänlihassolujen ionikanavageenien ilmentymistä tai niiden alleeli-ilmentymiseroja hyödyntämällä qPCR-menetelmää kolmessa erillisessä työssä. Ensimmäisessä työssä arvioitiin solulyysaukseen perustuvan genotyyppausmenetelmän soveltuvuutta sydänsolulinjojen karakterisointiin. Toisen työn tavoitteena oli arvioida alleeli-ilmentymiserojen vaikutuksia tautifenotyypin vaihteluun ja kehittymiseen. Kolmannen työn tarkoituksena oli tutkia yksisolu-qPCR-menetelmän tehokkuutta havainnoida yksittäisten sydänlihassolujen geeni-ilmentymistä.
Menetelmät: qPCR-menetelmää käytettiin jokaisessa työssä mittaamaan ionikanavageenien tai rakennegeenien mRNA-tasoja LQTS-spesifisistä sydänlihassoluista. Ensimmäisessä työssä käytettiin TaqMan® Sample-to-SNP™ Kit -menetelmää karakterisoimaan heterotsygoottisia sydänsolulinjoja, joissa oli *KCNQ1*-geenin mutaatio. Alleeli-ilmentymisvaihteluun perustuva tutkimus suoritettiin plasmideista tuotetun standardikuvaajan avulla jokaiselle Suomessa vallitsevalle perustajamutaatiolle. Viimeisessä työssä käytettiin Single cell-to-CT™ Kit -menetelmää, jonka avulla mitattiin *TNNT2*-geenin ilmentymistä sekä yksittäissolu- että solupopulaatiotasolla.
Tulokset: Ensimmäisen työn tuloksista pääteltiin, että solulyysaukseen perustuva genotyyppausmenetelmä soveltuu sydänsolulinjojen karakterisointiin, eikä analyysiä häiritseviä tekijöitä havaittu. Alleeli-ilmentymiseen perustuva tutkimus paljasti, että KCNQ1-FinA ja KCNQ1-FinB spesifisissä sydänlihassoluissa *KCNQ1*-geenin alleelit ilmentyivät 3:1-suhteessa, joka tarkoitti sitä, että villityyppialleelien ilmentyminen oli kolminkertainen verrattuna mutanttialleelien ilmentymiseen näissä LQT1-spesifisissä soluissa. Single cell-to-CT™ Kit -menetelmällä ei onnistuttu havainnoimaan *TNNT2*-geenin ilmentymistä yksittäissolutasolla ja solupopulaatiotasolla sen ilmentyminen oli myös heikkoa.
Johtopäätökset: Havaittu alleeli-ilmentymissuhde 3:1 (WT:MUT) KCNQ1-FinA ja KCNQ1-FinB mutatoituneissa sydänlihassoluissa voisi johtaa mutaatioiden heikentyneisiin fenotyyppivaikutuksiin, koska villityyppialleelin voimakkaampi ilmentyminen saattaa heikentää mutaatioiden vaikutuksia. Aiemmin on arveltu, että perustajamutaatioiden heikompi fenotyyppivaikutus on johtanut niiden yleistymiseen Suomessa. Tällöin taudinaiheuttajageenien alleelien ilmentymiserot saattavat vaikuttaa merkittävästi tautifenotyyppiin. Tämän varmistamiseksi on kuitenkin tutkittava alleeli-ilmentymiserot suuremmasta populaatiosta mutaationkantajia, joilla on havaittu suuri fenotyyppivaihtelu. Jos alleeli-imbalanssin ja fenotyypin välillä havaitaan korrelaatiota, voitaisiin alleeli-imbalanssi varmistaa yhdeksi fenotyyppivaihtelua selittäväksi geneettiseksi tekijäksi.

Abbreviations

AKAP	A-kinase anchoring protein
APD	action potential duration
bFGF	basic fibroblast growth factor
BMP-4	bone morphogenetic protein 4
cAMP	cyclic adenosine monophosphate
cDNA	complementary DNA
CPVT	catecholaminergic polymorphic ventricular tachyarrhythmia
Ct	threshold cycle
DAD	delayed after-depolarization
EAD	early after-depolarization
EB	embryonic body
ECG	electrocardiogram
END-2	visceral endoderm-like cell
ESC	embryonic stem cell
HCN	hyperpolarization-activated cyclic nucleotide-gated channel
HERG	human ether-a-go-go-related gene
iPSC	induced pluripotent stem cell
I_{Kr}	rapidly activating delayed rectifier K^+ current
I_{Ks}	slowly activating delayed rectifier K^+ current
JLNS	Jervell and Lange-Nielsen syndrome
Klf4	Krüppel-like factor 4
LQTS	long QT syndrome
LQT1	long QT syndrome type 1
LQT2	long QT syndrome type 2
MEA	microelectrode array
MiRP1	MinK-related peptide-1
MUT	mutant
Oct4	octamer-binding transcription factor 4
PAS	Per-Arnt-Sim domain
PBS	phosphate buffered saline
PCR	polymerase chain reaction
PKA	protein kinase A
PP1	protein phosphatase-1
qPCR	quantitative real-time polymerase chain reaction
QTc	QT interval corrected with heart rate
RPLP0	ribosomal protein, large, P0
RWS	Romano-Ward syndrome
RYR2	ryanodine receptor
SNP	single nucleotide polymorphism
Sox2	sex-determining region Y -box 2
TdP	Torsades de Pointes
TGF-β1	transforming growth factor β1
TNNT2	cardiac troponin T2
WNT	wingless/INT protein
WT	wild type

Table of Contents

1. Introduction

Long QT syndrome (LQTS) is a cardiac channelopathy causing life-threatening arrhythmias that can lead to sudden death at the young age (Roden et al., 2008). LQTS-associated mutations affect electrical function of cardiac ion channels resulting in delayed repolarization within cardiomyocytes that is observed as prolonged QT interval on the electrocardiogram measured from mutation carriers. There has been observed significant phenotypic variation and incomplete disease penetrance among LQTS patients that have led to suggestions that various genetic or non-genetic factors may modify disease phenotypes (Fodstad et al., 2004; Lahti et al., 2012). The unique enrichment of LQTS-specific founder mutations among Finnish population (Fodstad et al., 2004) offers enormous opportunity to evaluate factors affecting LQTS development and phenotypic variation.

The iPSC technology developed by Takahashi et al. (2007) produce a revolutionary approach to identify disease mechanisms in a novel way by allowing generation of disease-specific cell types derived from disease-causing mutation carriers, and thereby enabling more accurate *in vitro* disease modelling than was able with previous models. Many robust differentiation protocols have been developed to generate functional cardiomyocytes from patient-specific iPSCs (Mummery et al., 2012). They have increased generation of LQTS-specific disease models for allowing efficient evaluations of disease phenotypic features and drug responsiveness within cardiomyocytes containing various LQTS-related mutations (Itzhaki et al., 2011; Matsa et al., 2011). Furthermore, using iPSC-derived LQTS-specific cardiomyocytes, the unknown cellular mechanisms that cause variability for disease phenotypic features among patients can be examined.

2. Review of literature

2.1. Cardiac ion channels involving in development of action potential

In the sinoatrial node of the heart, pacemaker cardiomyocytes are able to spontaneously depolarize themselves developing electrical impulse that conducts throughout the heart (Giudicessi and Ackerman, 2012). Conduction system regulates motion of electrical impulse to the myocardium where electrical excitation initiates action potential development within cardiomyocytes (Bezzina and Wilde, 2007; Grant, 2009). Gap junctions between cardiomyocytes enable effective propagation of electrical excitation leading to contraction of the myocardium in order to ensure proper blood pumping ability of the heart (Giudicessi and Ackerman, 2012). This electrical function is detected on the surface electrocardiogram (ECG) (Bezzina and Wilde, 2007). On the ECG, P-wave indicates contraction of atria from which electrical impulse conducts along Purkinje fibers to ventricles. Depolarization of the ventricles forms QRS-complex and ventricular repolarization is detected as T-wave.

Cardiac ion channels and their rapid depolarizing and slow repolarizing ion currents (figure 1.) generate action potential in a response to electrical impulse. Action potential consists of resting (phase 4), depolarization (phase 0), transient repolarization (phase 1), plateau (phase 2) and repolarization (phase 3) steps (figure 1.) in which ion conductance through cardiac ion channels occurs along electrochemical gradients (Grant, 2009). The conduction of electrical impulse to the myocardium initiates depolarization of cardiomyocytes by activating sodium ion channels that lead to influx of Na^+ ions (Giudicessi and Ackerman, 2012). During depolarization phase, negative resting membrane potential becomes more positive due to increased intracellular Na^+ concentration via inward I_{Na} current. Depolarization is followed by a short, transient repolarization phase caused by outward potassium current, I_{to} through *KCND3*-encoded channels (Giudicessi and Ackerman, 2012). During the plateau phase, maintenance of positive membrane potential occur via inward current of Ca^{2+} ions and outward current of K^+ ions through L-type Ca^{2+} ion channels and delayed rectifier K^+ ion channels, respectively (Roden et al., 2002; Bezzina and Wilde, 2007). Increased intracellular Ca^{2+} concentration induces releasing of stored calcium ions from sarcoplasmic reticulum through ryanodine receptors (RYR2) (Bezzina and Wilde, 2007) and thereby further increasing Ca^{2+} concentration causes contraction of sarcomeres within cardiomyocytes.

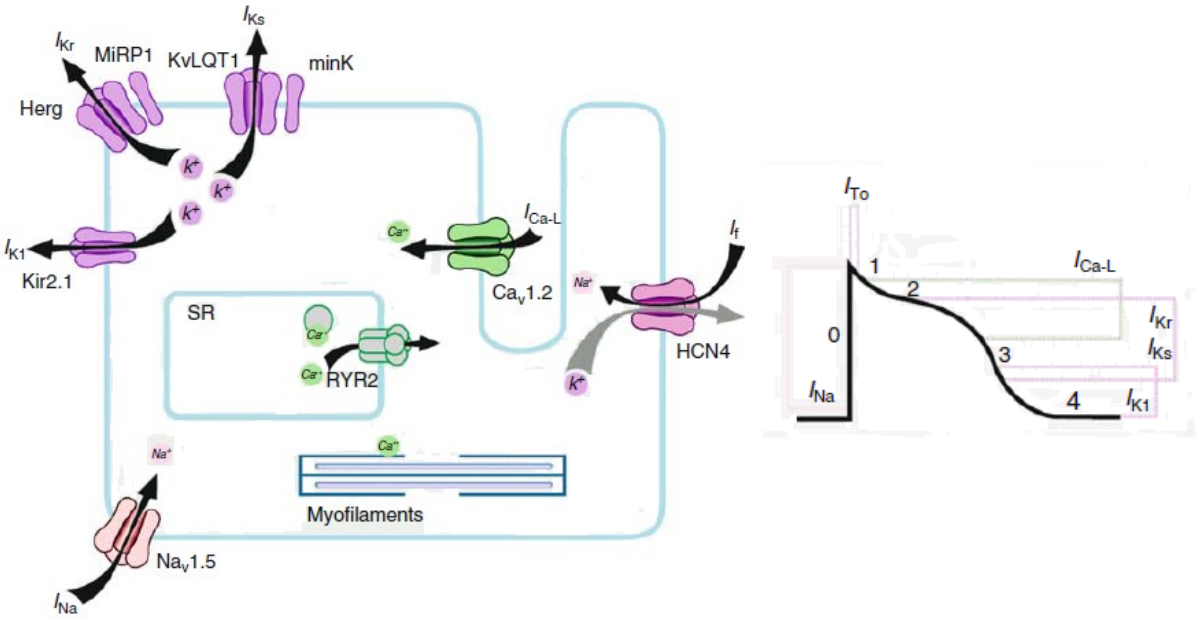

Figure 1. Schematic picture of a cardiomyocyte and its cardiac ion channels which involve in action potential development. Ion currents conducted by different cardiac ion channels during ventricular action potential are represented in the figure on the right. Sequential ion conductions of the channels ensure appropriate electrical function of a cardiomyocyte leading to its contraction. The figures were modified from origin Bezzina and Wilde, 2007.

Activation of outward potassium ion channels occurs during plateau phase and they are responsible for cardiomyocyte repolarization (Bezzina and Wilde, 2007). Repolarizing K^+ ion currents restore negative resting membrane potential that is -80 mV in atrial and -85 mV in ventricular cardiomyocytes (Giudicessi and Ackerman, 2012). In addition, variation in action potential durations (APD) and configurations are seen between nodal, atrial and ventricular cardiomyocytes due to different functional ion channels and proteins associated with them (Roden et al., 2002). Termination of repolarization and maintenance of resting membrane potential are occurred by outward K^+ ion current, I_{K1} through inward rectifier potassium channel encoded by *KCNJ2* gene (Tristani-Firouzi et al., 2002; Bezzina and Wilde, 2007). When resting membrane potential has recovered and contraction has relaxed, new electrical excitation can initiate development of action potential within myocardium. Pacemaker current, I_f depolarizes nodal cardiomyocytes in the sinoatrial node, leading to generation of new electrical impulse (Amin et al., 2010). I_f-conducting channels are hyperpolarization-activated cyclic nucleotide-gated (HCN) channels indicating that hyperpolarization triggers their activation and intracellular cyclic adenosine monophosphate (cAMP) levels regulate their current amplitudes (Amin et al., 2010).

Voltage-gated cardiac Na^+ and Ca^{2+} ion channels conduct depolarizing ion currents, I_{Na} and I_{Ca}, respectively, which change normal negative membrane potential to more positive during action potential (Giudicessi and Ackerman, 2012). These channels share structural similarity. Both channels compose of single α-subunit encoded by *SCN5A* or *CACNA1C*, respectively, that contains four homologous domains and each includes six transmembrane segments (Grant, 2009; Amin et al., 2010). Pore-forming loop locates between S5 and S6 segments in each domain and its amino acid content specifies selectivity of ion conductance (Bezzina and Wilde, 2007). Voltage-gating of cardiac ion channels is based on voltage sensing S4 segments which react to changes in membrane potential by altering open and close conformations of channel due to their content of positively charged amino acid residues, including arginine or lysine in every third position (Roden et al., 2002; Grant, 2009).

In cardiomyocytes, two potassium ion channels are active in repolarization phase and they regulate action potential duration (APD) (Bezzina and Wilde, 2007). *KCNQ1* gene encodes α-subunits of slowly activating delayed rectifier K^+ ion channels that conduct I_{Ks} currents (Vincent, 1998; Jespersen et al., 2005). The other repolarizing ion current is I_{Kr} conducted by rapidly activating delayed rectifier K^+ ion channels that compose of α-subunits encoded by *KCNH2* gene (known also as human ether-a-go-go-related gene, *HERG*) (Vincent, 1998; Roden et al., 2002). Structures of these voltage-gated potassium ion channels (figure 2.) resemble Na^+ and Ca^{2+} ion channels but they contain four α-subunits assembled to tetrameric structure (Bezzina and Wilde, 2007). Each α-subunit has six transmembrane segments that have similar functions as described above. Four α-subunits organize to form pore region to the middle of ion channel that is surrounded by α-helices of S6 segments (Bezzina and Wilde, 2007). When the channel is inactivated, S6 segments have oriented across each other and prevent K^+ ion permeation (Sanguinetti and Tristani-Firouzi, 2006). Depolarization induces movement of S6 segments resulting in increased size of pore region allowing ion conduction. The amino acid contents responsible for K^+ ion selectivities are Gly-Tyr-Gly (Grant, 2009) and Ser-Val-Gly-Phe-Gly (Sanguinetti and Tristani-Firouzi, 2006) in KCNQ1 channel and HERG channel, respectively.

Both repolarizing cardiac K^+ ion channels interact with auxiliary β-subunits that are required for properly formed functional channels. *KCNE1*-encoded MinK β-subunit interacts with

slowly activating delayed rectifier K^+ ion channel (Splawski et al., 1997) and modifies its gating properties by slowing channel activation and deactivation and reducing inactivation that result in increased I_{Ks} current (Jespersen et al., 2005). The suggested number of interacting MinK subunits with KCNQ1 channel is two or four locating close to pore-forming region (Jespersen et al., 2005). *KCNE2*-encoded MiRP1 (MinK-related peptide-1) interacts with rapidly activating delayed rectifier K^+ ion channel (Abbott et al., 1999). MiRP1 alter HERG channel gating by slowing activation and increasing deactivation rates. Therefore, HERG channels open in a response to higher positive membrane potential caused by depolarization and return more rapidly to deactivate state after repolarization (Abbott et al., 1999). MinK and MiRP1 share significant sequence similarity, reflecting to their functional similarities among K^+ ion channels (Abbott et al., 1999; Jespersen et al., 2005). For example, MinK β-subunit is able to interact with HERG channel as well, but it cannot alter that channel gating similarly than MiRP1 does (Abbott et al., 1999).

Many cardiac ion channels are closed by deactivation, indicating that open channels close rapidly when the membrane potential is near to threshold potential (Grant, 2009). The deactivation is the most critical process because if it has accelerated or slowed the influence reflects directly to APD (Abbott et al., 1999; Clancy and Rudy, 2001). Gating properties of HERG channels are unique as compared to other cardiac ion channels (Clancy and Rudy, 2001; Sanguinetti and Tristani-Firouzi, 2006). Cardiomyocyte depolarization induces extremely rapid transition of HERG channels from open state to inactivated state. During plateau phase, positive membrane potential is increasing and that triggers opening of inactivated channels allowing greater amplitude of I_{Kr} current and initiation of cardiomyocyte repolarization. Deactivation of HERG channels occurs slowly for ensuring sufficient repolarization. Similar rapid inactivation process does not occur among other cardiac ion channels during action potential (Amin et al., 2010).

Insufficient or abnormal cardiac ion channel function can lead to development of arrhythmic disease state that have been characterized within various disorders, such as long QT syndrome, short QT syndrome, Brugada syndrome and catecholaminergic polymorphic ventricular tachycardia (CPVT) (Kontula, 2005; Bezzina and Wilde, 2007). Structural abnormalities or defective electrical function affect conductance ability of ion channels

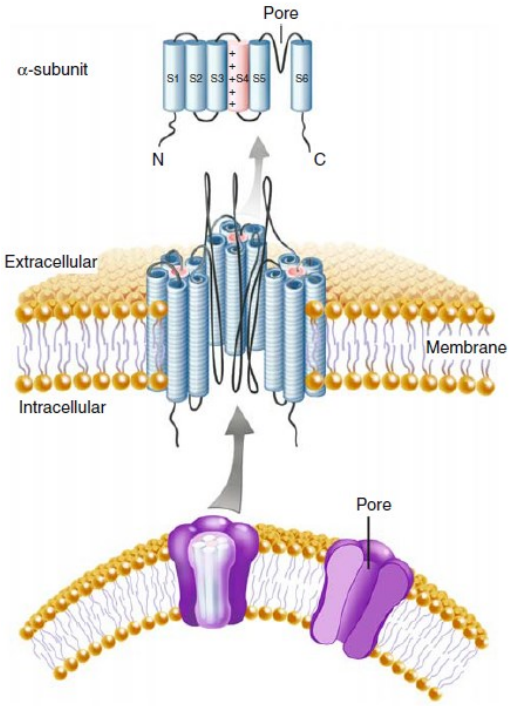

Figure 2. Structure of voltage-gated potassium ion channel in cardiomyocytes. K^+ ion channels consist of four α-subunits containing six transmembrane segments. The pore region formed by assembled α-subunits is surrounded by loop structures between S5 and S6 segments. S4 segment is responsible for sensing voltage changes leading to channel opening or closing during action potential. Similar membrane organizations are observed in sodium and calcium ion channels, but they are composed by single α-subunit containing four domains, resembling represented α-subunit. The figure was modified from the origin Bezzina and Wilde, 2007.

resulting in altered action potential within cardiomyocytes and increased risk of arrhythmias (Roden et al., 2002). Early after-depolarizations (EADs) and delayed after-depolarizations (DADs) are common mechanisms to develop arrhythmias caused by altered ion channel functions during action potential. Prolonged action potential duration can reactivate L-type Ca^{2+} ion channels leading to spontaneous depolarization of cardiomyocytes and development of EADs (Vincent, 1998; Clancy and Rudy, 2001; Amin et al., 2010). Generation of DADs can occur if increased intracellular Ca^{2+} concentration, due to the reactivated channels, causes release of Ca^{2+} ions from sarcoplasmic reticulum in order to prepare cardiomyocyte to contract (Saucermann et al., 2004), or if Na^+ ion channels become activated during resting phase due to activated Na^+/Ca^{2+}-exchangers which remove excess intracellular calcium while increase intracellular sodium levels (Amin et al., 2010). EADs and DADs may trigger development of ventricular tachyarrhythmias that can lead to sudden cardiac death (Vincent, 1998).

2.2. Long QT syndrome

Long QT syndrome is a congenital heart disease causing severe arrhythmias associated with increased risk of sudden death at the young age (Vincent, 1998; Roden, 2008). The LQTS is characterized by prolonged QT interval observed on the ECG measurement. The QT interval describes development of ventricular action potential and its duration (Grant, 2009) and therefore LQTS induces prolongation of ventricular repolarization phase within cardiomyocytes. LQTS-associated ventricular arrhythmias and specific polymorphic ventricular tachycardia, known as *torsades de pointes* (TdP), can lead to ventricular fibrillation and sudden death caused by cardiac arrest (Vincent, 1998; Roden, 2008; Toivonen et al., 2008). Common clinical manifestations related to LQTS are syncopes and seizures resulted from cardiac events that are usually detected at childhood or adolescence (Vincent, 1998).

The most prevalent form of LQTS is autosomal dominantly inherent Romano-Ward syndrome (RWS) (Splawski et al., 2000; Bezzina and Wilde, 2007) which clinical prevalence in worldwide ranges between 1:5000 – 1:10000 (Fodstad et al., 2004; Marjamaa et al., 2009), but in Finland the clinical prevalence is 1:3000 (Toivonen et al., 2008) that is relatively higher than has been characterized within other populations. The RWS is caused by heterozygous mutations in genes encoding subunits of cardiac ion channels or proteins which assist their functions. LQTS-associated gene mutations either increase depolarizing inward I_{Na} or I_{Ca} currents or reduce repolarizing outward I_{Ks}, I_{Kr} or I_{K1} currents that result in prolonged ventricular repolarization and increased APD leading to prolongation of QT interval seen on patient's ECG (Bezzina and Wilde, 2007; Giudicessi and Ackerman, 2012). More than 400 LQTS-causing mutations have been identified (Ackerman, 2005) and 75 % of the diagnosed patients have mutation in one of the *KCNQ1*, *KCNH2* or *SCN5A* genes (Marjamaa et al., 2009) which cause the most common subtypes of LQTS: LQT1, LQT2 and LQT3, respectively. Romano-Ward syndrome type LQTS has been divided into twelve subtypes (Amin et al., 2010) according to the gene affected by disease-causing mutation (table 1). Eight of the subtypes are caused by mutations in genes encoding either α- or β-subunits of the cardiac ion channels. The rest four subtypes have been identified to be caused by mutations in proteins assisting ion channel functions (table 1.). Ion channel defects caused by mutations are primary affecting the function of the heart, but subtypes LQT7 (Tristani-Firouzi et al., 2002) and LQT8 (Splawski et al., 2004) are characterized by distinct physiological and

developmental dysfunctions in multiple organs besides to cardiac events and prolonged QT interval. Each subtype produces different T-wave morphology on the ECG and it can be used for their identification or prediction of underlying disease-causing gene mutations (Vincent, 1998; Ackerman, 2005).

The more rare form of LQTS is autosomal recessively inherent Jervell and Lange-Nielsen syndrome (JLNS) having incidence as low as 1:500 000 (Splawski et al., 1997). The JLNS is caused by homozygous mutations in *KCNQ1* (Neyroud et al., 1997; Splawski et al., 1997) or *KCNE1* (Schulze-Bahr et al., 1997) genes. Compared with RWS, disease phenotype in JLNS is more severe, including sensorineural deafness and more increased risk of sudden death (Neyroud et al., 1997) due to that homozygous mutations cause significant suppression of channel subunit expression (Schmitt et al., 2000). In addition to cardiac expression of *KCNQ1* and *KCNE1*genes, they are expressed in marginal cells of stria vascularis in inner ear where ion channels encoded by them transport K^+ ions into endolymph (Neyroud et al., 1997). Therefore impaired ion transportation of mutated channels cause decreased K^+ concentration of the endolymph lead to inner ear defects.

Diagnosis of long QT syndrome is based on measured time of QT interval by the ECG and experienced LQTS-related symptoms, such as palpitations, ventricular arrhythmias, syncope caused by physical effort, stress or unexplainable reason, undetected structural aberration in heart, or some family member has LQTS diagnosis (Vincent, 1998; Bezzina and Wilde, 2007; Saenen and Vrints, 2008; Toivonen et al., 2008). However, prolonged QT interval cannot be used alone for basis of LQTS diagnosis because even 40-50 % mutation carriers do not have difference in length of QT interval when compared to healthy people (Vincent, 1998). QT interval corrected with heart rate (QTc) is better parameter than QT interval directly detected on the ECG for evaluating the prolongation due to that the heart rate impacts significantly on the length of QT interval (Bezzina and Wilde, 2007). Thereby, differences in heart rhythms within population can be compensated by using QTc values. To calculate QTc values Bazett's formula is used: $QTc\ (ms) = QT\ (ms) / \sqrt{RR\ (s)}$. Prolonged QTc is defined to be over 450 ms in men and over 460 ms in women (Giudicessi and Ackerman, 2012). However, the only option to verify diagnosis is genetic analysis in order to identify underlying gene mutation (Toivonen et al., 2008) because high variability of symptoms among LQTS patients

Table 1. Long QT syndrome subtypes.

Long QT syndrome subtype	Gene and its locus*	Protein and its function	Pathological mechanism of mutation for ion channel function	References
LQT1	KCNQ1, 11p15.5	K_V7.1, α-subunit of slowly activating delayed rectifier K^+ ion channel	Decrease outward I_{Ks} by many mechanisms, e.g. affecting assembly ability of α-subunit, altering gating properties and reducing trafficking	Piippo et al., 2001; Moretti et al., 2010
LQT2	KCNH2, 7q36.1	K_V11.1, α-subunit of rapidly activating delayed rectifier K^+ ion channel	Decrease outward I_{Kr} by accelerating deactivation rate	Fodstad et al., 2006
LQT3	SCN5A, 3p21	Na_V1.5, α-subunit of Na^+ ion channel	Increase inward I_{Na} by delaying rapid channel inactivation and causing reopenings at depolarization phase	Splawski et al., 2000
LQT4	ANK2, 4q25-q27	Ankyrin-B, membrane adapter protein	Reduced ankyrin-B decrease protein levels and cellular organization of Na/K ATPase, Na/Ca exchanger and inositol-1,4,5-trisphosphate receptor resulting in increased intracellular Ca^{2+} concentrations	Mohler et al., 2003
LQT5	KCNE1, 21q22.12	MinK, β-subunit of KCNQ1-encoded ion channel	Decrease outward I_{Ks} by increasing required voltage for channel activation and accelerate deactivation rate	Splawski et al., 1997
LQT6	KCNE2, 21q22.12	MiRP1, β-subunit of KCNH2-encoded ion channel	Decrease outward I_{Kr} by increasing required voltage for channel activation and accelerate deactivation rate	Abbott et al., 1999
LQT7 (Andersen syndrome)	KCNJ2, 17q24.3	Kir2.1, α-subunit of inward rectifier K^+ ion channel	Decrease outward I_{K1} by causing reduction in extracellular K^+ concentration and prolongation of terminal repolarization	Tristani-Firouzi et al., 2002
LQT8 (Timothy syndrome)	CACNA1C, 12p13.3	Ca_V1.2, α-subunit of L-type Ca^{2+} ion channel	Increase inward I_{Ca} by slowing channel inactivation rate resulting in increased intracellular Ca^{2+} concentration	Splawski et al., 2004
LQT9	CAV3, 3p25	Caveolin-3, component of caveolae which associates with Na^+ ion channels	Increase inward I_{Na} by causing gain of function of Na^+ ion channel	Vatta et al., 2006
LQT10	SCN4B, 11q23.3	β4, one of the auxiliary β-subunits of Na^+ ion channel	Increase inward I_{Na} by modifying channel inactivation	Medeiros-Domingo et al., 2007
LQT11	AKAP9, 7q21-q22	Yotiao, mediate phosphorylation of KCNQ1-encoded K^+ ion channel with protein kinase A	Disrupted phosphorylation of KCNQ1 channel reduces I_{Ks} during β-adrenergic stimulation	Chen et al., 2007
LQT12	SNTA1, 20q11.2	α1-syntrophin, regulates interaction between Na_V1.5 and nNOS-PMCA4b complex	Increase inward I_{Na} by preventing function of PMCA4b resulting in increased direct S-nitrosylation of Na_V1.5	Ueda et al., 2008

* indicates that data of genetic loci has been searched from Gene database of NCBI (http://www.ncbi.nlm.nih.gov/gene, cited on 5.4.2015).

complicates identification of robust disease phenotype. In addition, due to highly family specific feature of LQTS-associated mutations (Fodstad et al., 2004), genetic testing allows screening of symptomless mutation carriers within families with diagnosed LQTS.

The treatment of LQTS patients is decided according to occurrence of cardiac events. All symptomatic patients, and usually many asymptomatic patients too, are treated with β-blockers in order to prevent cardiac events and TdPs, but the highest benefit of this treatment is achieved in LQT1 due to its associated β-adrenergic stimulus trigger (Vincent, 1998; Bezzina and Wilde, 2007). The common treatments for patients having severe cardiac events regardless of β-blocker medication are pacemaker or implantable cardiac defibrillator (Saenen and Vrints, 2008) which maintain the normal heart rhythm and inhibit occurrence of ventricular arrhythmias.

Incomplete disease penetrance and phenotypic variations within LQTS patients is significantly common (Fodstad et al., 2004; Lahti et al., 2012). Some affected individuals have experienced severe cardiac symptoms whereas many patients are completely asymptomatic and not even aware that they carry disease-causing mutation (Lahti et al., 2012). Approximately even half of the diagnosed patients are symptomless (Toivonen et al., 2008), indicating high variation in the clinical manifestation among diagnosed patients. Furthermore, it is typical that disease phenotype varies within family with the same mutation in a particular gene (Fodstad et al., 2006). Due to high phenotypic variation and many not diagnosed asymptomatic patients, the determination of prevalence is difficult and the risk of misdiagnosis increase (Egashira et al., 2012). It has been estimated that the amount of LQTS patients with undetected disease-causing mutation is approximately 20 % (Vatta et al., 2006; Ueda et al., 2008). There have been suggested that some genetic or non-genetic factors are affecting for development of variable disease phenotypes (Piippo et al., 2001; Fodstad et al., 2006) and their identification could enhance knowledge about factors provoking severe form of LQTS or which factors cause completely asymptomatic form.

One type of LQTS is acquired or drug-induced form in which cardiac events are caused by QT interval prolonging drugs. These kinds of drugs block I_{Kr} currents in HERG potassium ion

channels due to their specific structures of extracellular pore region which make them highly susceptible to be blocked (Roden et al., 2002; Sanguinetti and Tristani-Firouzi, 2006). Two structural features have been identified to increase HERG channel susceptibility (Roden et al., 2002; Sanguinetti and Tristani-Firouzi, 2006). Lack of prolines in S6 segments result in enlarged pore region which is more susceptible for drug blockade when compared to other K^+ channels in which prolines cause their twisting and therefore reducing pore region size. Second reason is that pore region of HERG channels contain aromatic amino acids (Tyr652 and Phe656) which can bind with charged or aromatic residues of drugs allowing more sustained blockade. Many cardiac and non-cardiac, such as some antihistamine, antibiotic and psychotropic (Vincent, 1998), drugs are able to prevent ion conducting function of HERG channel. Defective function resulted from drug blockade lead to increased risk of development of arrhythmias and other cardiac events (Lahti et al., 2012). That is why LQTS patients have to avoid drugs that could prolong QT interval.

2.2.1. Mutations causing long QT syndrome

LQTS-associated mutations are located in genes encoding α- or β-subunits of cardiac ion channels (Splawski et al., 2000) or their auxiliary proteins, such as ankyrin-B (Mohler et al., 2003) and Yotiao (Chen et al., 2007). Until now, twelve genes have been identified to increase susceptibility for LQTS when containing specific mutations (Amin et al., 2010) by either reducing repolarizing K^+ currents or increasing depolarizing Na^+ or Ca^{2+} currents that result in abnormal electrical function of cardiomyocytes and increased risk of development of arrhythmias (Bezzina and Wilde, 2007). Although strong family history is related to LQTS and many mutations are highly family specific, LQTS-causing rare de novo mutations have also been identified (Splawski et al., 2004; Vatta et al., 2006). Loss-of-function mutations with dominant negative effects are common among LQTS-causing mutations, especially within K^+ ion channels, and usually those cause significant reductions of affected ion currents (Clancy and Rudy, 2001), and therefore higher risk of severe disease phenotype (Moss et al., 2007).

Important property of KCNQ1 channel is the response for β-adrenergic stimuli and accelerated heart rate resulted from e.g. physical exercise by increasing repolarizing K^+ current amplitude (Bezzina and Wilde, 2007; Giudicessi and Ackerman, 2012). However, mutated channels are not able to react sufficiently to increased depolarizing currents caused

by β-adrenergic stimulation, and that lead to occurrence of LQT1-related cardiac symptoms during exercise or emotional stress and not typically seen shortening of QT interval.

There are three main mechanisms how LQTS-associated mutations affect functions of cardiac ion channels. Mutations may cause defective assembly ability of subunits resulting in impaired formation of functional channels (Schmitt et al., 2000). This mechanism has been identified from K^+ ion channels having tetrameric structure of four α-subunits. When allelic expression of mutant and wild type alleles are equal, the reduction of K^+ current could be expected to be 50 % (Bezzina and Wilde, 2007). However, many LQTS-causing mutations have dominant negative effects, indicating that only single mutant α-subunit involving in channel-forming tetramer can cause channel dysfunction. Therefore reduction of ion current could be more than 50 % in mutated channels (Moss et al., 2007; Saenen and Vrints, 2008). The other common pathogenic mechanism is altered channel gating or kinetics that affect directly to ion conductance of channels (Bezzina and Wilde, 2007). In addition, reduced trafficking of mutant subunits from endoplasmic reticulum to cell membrane of cardiomyocytes decrease amount of surface expressed channel-forming subunits (Clancy and Rudy, 2001; Sanguinetti and Tristani-Firouzi, 2006). Mutations can change protein synthesis or folding of translated proteins leading to their impaired trafficking (Sanguinetti and Tristani-Firouzi, 2006) or mutation can suppress directly the protein trafficking (Moretti et al., 2010). For example, defective protein trafficking has been identified to be major reason for abnormal function of HERG channels affected by 80-90 % of LQTS-associated *KCNH2* gene mutations (Giudicessi and Ackerman, 2012).

Risk of occurrence of cardiac events and their severities are significantly dependent on mutation type and location within subunits of cardiac ion channels (Giudicessi and Ackerman, 2012). 72 % of LQTS-associated mutations are missense mutations causing change of single amino acid residue in subunit or auxiliary proteins (Splawski et al., 2000). Their phenotypic effects are highly dependent on location. If the mutation locates in region that has important role in ion channel function, the LQTS-related phenotypic effects are more severe (Toivonen et al., 2008). Especially influences of mutation locations within potassium ion channels encoded by *KCNQ1* and *KCNH2* genes have been evaluated (Giudicessi and Ackerman, 2012). LQT1-causing mutations have been associated with increased risk of cardiac events,

more severe disease phenotype and longer QT interval if a mutation locates in transmembrane domains or C-terminal part of α-subunit because those parts have effects on gating properties and subunit assembly ability, respectively. LQT2-associated mutations increase susceptibility for LQTS phenotype if they locate in pore-forming region, including S5 and S6 segments and pore-forming loop between them, resulting in altered K^+ transportation and channel gating (Splawski et al., 2000). In addition, N-terminal location of mutation is associated with accelerated deactivation of HERG channel (Splawski et al., 2000; Clancy and Rudy, 2001). However, mutations that have stronger influence to protein structure (e.g. frame-shift mutations, insertions and deletions) cause always severe phenotypes despite of their locations (Giudicessi and Ackerman, 2012).

2.2.1.1. LQTS-associated mutations in Finland

Four founder mutations that cause long QT syndrome have been identified to be predominating in Finland, indicating that 73 % of diagnosed LQTS patients among Finnish population carry one of the four disease-causing founder mutation (Fodstad et al., 2004). Two of them are located in *KCNQ1*-encoded α-subunit (figure 3.) and are named as KCNQ1-FinA (G589D) (Piippo et al., 2001) and KCNQ1-FinB (IVS7-2A>G) (Fodstad et al., 2006). They cause LQT1 subtype that is the most common (71 %) subtype occurring in Finland and elsewhere (Fodstad et al., 2004). The remaining two mutations are HERG-FinA (L552S) (Piippo et al., 2000) and HERG-FinB (R176W) (Laitinen et al., 2000; Fodstad et al., 2006) locating in *KCNH2*-encoded α-subunit (figure 3.) and causing LQT2 subtype which proportion from Finnish LQTS cases is 20-30 % (Fodstad et al., 2004). Marjamaa et al. (2009) estimated that the prevalence of founder mutations within Finnish population may be even 1:250, indicating their significant enrichment as compared to relatively lower prevalences of LQTS-associated mutations in worldwide and other estimations from Finland (Fodstad et al., 2004). Despite of high prevalence, only approximately 20-30 % of mutation carriers have cardiac events related to LQTS (Marjamaa et al., 2009) and that may be resulted from milder effects of founder mutations that have allowed their enrichment within Finnish population (Piippo et al., 2001).

KCNQ1-FinA (G589D) is a missense mutation which has position in C-terminal part of the KCNQ1 protein. Genetic location of the mutation is in nucleotide 1876 where normally occurring guanine has changed to adenine causing substitution of glycine by aspartic acid at

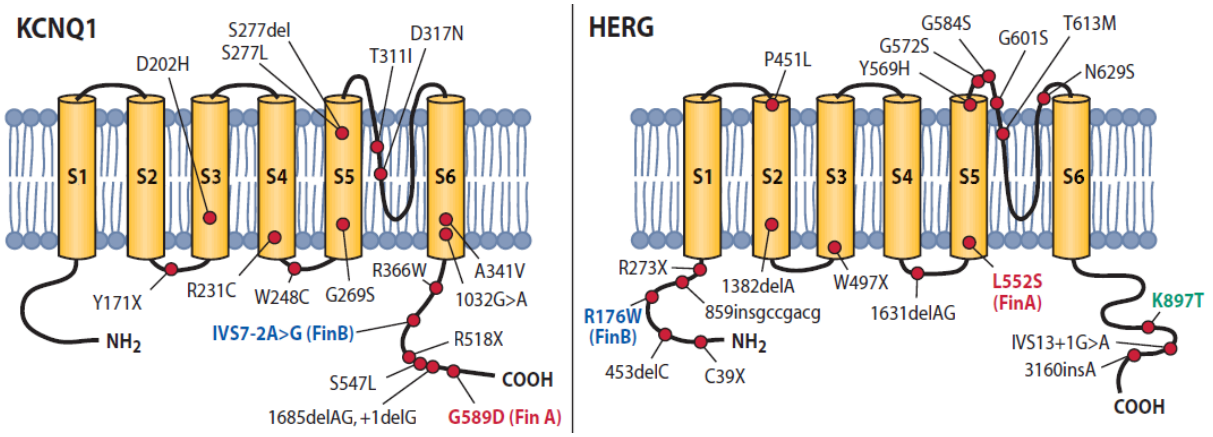

Figure 3. Locations of four Finnish founder mutations in K^+ ion channels' α-subunits encoded by *KCNQ1* and *KCNH2* genes. KCNQ1-FinA and KCNQ1-FinB mutations locate in C-terminal part of KCNQ1 protein. In HERG protein, locations of HERG-FinA and HERG-FinB are in S5 segment and N-terminal part, respectively. FinA mutations are marked by red and FinB mutations by blue. Other LQTS-causing mutations, represented in the figures, have also been identified from Finnish population in the study published by Fodstad et al. (2004). K897T in HERG protein is commonly occurring polymorphism identified from Finnish population and therefore it is highlighted with green in the figure. The figure was modified from the origin Kontula, 2005.

position 589 in KCNQ1 protein (Piippo et al., 2001). This mutation is the most common within all four founder mutations (Marjamaa et al., 2009). *KCNQ1*-encoding α-subunit has C-terminal subunit assembly domain at position 589-620, that has been identified to be essential for formation of functional tetrameric channels (Schmitt et al., 2000). Thus, mutations, such as KCNQ1-FinA, in that region cause abnormal function of assembly domain resulting in disability of α-subunit to assemble with other subunits generally in dominant negative manner (Schmitt et al., 2000; Piippo et al., 2001). Functional *in vitro* studies have revealed reduction of I_{Ks} current and increased required voltage for activation in KCNQ1-FinA mutated channels when they are expressed with MinK β-subunits (Marjamaa et al., 2009). Commonly detected reductions of I_{Ks} currents are approximately 50 % (Saucermann et al., 2004). In Finland have also been diagnosed few JLNS cases caused by homozygous KCNQ1-FinA mutations, but their prevalence is significantly lower than RWS caused by heterozygous mutations (Piippo et al., 2001).

Other mechanism that develops arrhythmic phenotype in LQT1 due to G589D-mutated KCNQ1 has been related to prevented β-adrenergic stimulation of mutant channel

(Saucermann et al., 2004). C-terminal location of KCNQ1-FinA mutation in α-subunits disrupts interaction between KCNQ1 channel and A-kinase anchoring protein (AKAP), Yotiao. Yotiao binds with two regulatory subunits of protein kinase A (PKA) and protein phosphatase-1 (PP1) to form signaling complex which mediates phosphorylation of KCNQ1 channel (Saucermann et al., 2004; Jespersen et al., 2005). The β-adrenergic stimulation increases intracellular cAMP levels leading to activation of PKA in the Yotiao and phosphorylation of N-terminal residue S27 in KCNQ1 α-subunit (Jespersen et al., 2005). Phosphorylated channel reacts on β-adrenergic stimulation by shortening action potential duration. But in the mutated KCNQ1 channels, phosphorylation does not occur because the mutation prevents α-subunits to interact with the Yotiao resulting in abnormal response for β-adrenergic stimuli. Therefore, mutated KCNQ1 channels cannot increase repolarizing I_{Ks} current at the same rate than I_{Ca} current is increasing during β-adrenergic stimulation that lead to QT interval prolongation and development of cardiac symptoms (Saucermann et al., 2004). Additionally, there has been identified mutation in the KCNQ1 binding domain of Yotiao resulting in LQTS-related phenotype and it has determined to cause LQT11 subtype (Chen et al., 2007). The mutation in Yotiao affects similarly to KCNQ1 channel than KCNQ1-FinA mutation by reducing phosphorylation and channel's response to increased cAMP levels.

KCNQ1-FinB (IVS7-2A>G) is an acceptor site mutation which cause insertion of 30 or 33 base pairs into the *KCNQ1* gene by eliminating splicing site between exons 7 and 8 (Fodstad et al., 2006). The IVS7-2A>G-mutated transcripts are translated into KCNQ1 α-subunits containing inserted 10 (Val-Thr-Ala-Cys-Pro-Pro-Ala-Arg-Pro-Arg) or 11 (contain added glutamine in front of valine) amino acids from the end of intron 7 into the C-terminal part of the protein. Functional *in vitro* studies have revealed loss-of-function and dominant negative features of the KCNQ1-FinB resulting in reduction of I_{Ks} current in KCNQ1 channel and significantly prolonged QT interval in affected patients (Fodstad et al., 2006; Marjamaa et al., 2009).

HERG-FinA (L552S) mutation causes nucleotide change from thymine to cytosine at position 1655 in the *KCNH2* gene that leads to substitution of leucine by serine at position 552 in the HERG protein (Piippo et al., 2000; Splawski et al., 2000). The mutation locates in cytoplasmic end of S5 segment which is known to be important in regulation of deactivation

and inactivation of HERG channel (Piippo et al., 2000). Therefore, the HERG-FinA mutation affects especially gating properties of the channel. Piippo et al. (2000) found that the mutation reduces I_{Kr} current by increasing channel activation and deactivation rates. In addition, they identified Finnish homozygote HERG-FinA carriers with more severe disease phenotypes than heterozygote carriers have, as have been observed in JLNS cases caused by homozygous *KCNQ1* and *KCNE1* mutations.

Laitinen et al. (2000) identified R176W mutation from *KCNH2* gene but its founder mutation nature occurring in Finland was revealed by Fodstad et al. (2006) and it was named as HERG-FinB. It is a missense mutation causing nucleotide change from cytosine to thymine in nucleotide 526 in *KCNH2* gene (Laitinen et al., 2000) resulting in substitution of arginine by tryptophan in N-terminal part of the HERG subunit (Fodstad et al., 2006; Lahti et al., 2012). The HERG-FinB mutation increases deactivation rate of HERG channel due to nearby location with PAS (Per-Arnt-Sim) domain which is known to slow channel deactivation rate (Clancy and Rudy, 2001; Fodstad et al., 2006). When deactivation is accelerated the ability of the channel to conduct K^+ ions is reducing that lead to prolonged repolarization of cardiomyocytes. One explaining factor for decreased I_{Kr} current is reduced trafficking of mutated α-subunits to the cell membrane resulting in lower amount of channel-forming α-subunits in the membrane, because HERG-FinB mutated subunits are still able to interact with normal subunits and form tetrameric ion channels (Fodstad et al., 2006). However, Fodstad et al. (2006) suggested that HERG-FinB may have milder effect on disease phenotype than other LQTS-associated mutations because there was not detected significant difference between current densities of wild type α-subunits and coexpressed wild type and HERG-FinB mutated subunits. In addition, they observed that compound heterozygosity was relatively common among HERG-FinB mutation carriers, indicating that they have other LQTS-associated mutation along with HERG-FinB, and therefore, the HERG-FinB may increase the risk of occurrence of cardiac symptoms in these disease cases.

Specific genetic spectrum has been related to LQTS-associated mutations in Finland, although LQTS-causing founder mutations have also been identified in Norway and South Africa (Fodstad et al., 2004). Geographical, linguistic, cultural and immigrational reasons have led to isolation of Finnish population during the history and that have enabled development and

enrichment of unique founder mutations (Piippo et al., 2000; Piippo et al., 2001; Fodstad et al., 2004). Founder mutations characterized from *KCNQ1* gene have only been identified among Finnish population but HERG-related mutations have also been diagnosed within other populations (Marjamaa et al., 2009). Geographical distribution of founder mutations can reveal information about their development and origin (Kontula, 2005). There have been observed evident geographical clustering of birthplaces of ancestors affected by Finnish founder mutations (Piippo et al., 2001; Fodstad et al., 2004), but nowadays, any clustering within mutation carriers cannot be characterized (Marjamaa et al., 2009).

2.3. Induced pluripotent stem cells

Induced pluripotent stem cells (iPSC) are generated from somatic cells by returning them into pluripotent state by reprogramming (Takahashi and Yamanaka, 2006; Takahashi et al., 2007; Yu et al., 2007). Takahashi and Yamanaka (2006) developed the iPSC technology for intend to replace need of embryonic stem cells (ESCs) in research field by cells which have similar properties. They succeeded in producing pluripotent stem cells from mouse fibroblasts and later from human fibroblasts (Takahashi and Yamanaka, 2006; Takahashi et al., 2007). The reprogramming is occurred by viral transduction of somatic cells with a combination of four transcription factors, including either Oct4, Sox2, Klf4 and c-Myc (Takahashi et al., 2007) or Oct4, Sox2, Nanog and Lin28 (Yu et al., 2007), that are maintaining pluripotency within ESCs. During reprogramming, delivered exogenous transcription factors modify gene expression of somatic cells through remodeling epigenetic features of DNA that lead to activation of expression of endogenous pluripotency-associated genes while expression of genes associated with differentiation is suppressed (Takahashi et al., 2007). The exogenous transgene expression has silenced within generated iPSCs and active endogenous pluripotency genes maintain their returned properties related to pluripotent state.

Many morphological and functional similarities between human iPSCs and human ESCs have been identified (Takahashi et al., 2007 ; Yu et al., 2007), such as similar colonies formed in *in vitro* cultures, equal self-renewal capacity and similar expression of pluripotency-related genes and surface markers. Both of them are able to differentiate into all cell types found in three germ layers: endoderm, mesoderm and ectoderm, and the differentiation capacity to create their derivatives are confirmed with *in vitro* formation of embryonic bodies (EB) and *in vivo* formation of teratomas (Lahti et al., 2012). However, isolation of ESCs from inner cell

mass of blastocyst causes ethical concerns considering the use of human embryos in researches (Takahashi and Yamanaka, 2006). In addition, ESCs are associated with a risk of immunological rejection. These problems can be avoided by using induced pluripotent stem cells instead. One great advantage of iPSCs is opportunity to generate patient- and disease-specific cells that contain identical genome with individual whose somatic cells have been used for iPSC generation (Zwi et al., 2009).

The iPSC-derived patient- and disease-specific cells have led to development of novel and efficient approach for disease modelling and drug development because previously only models used for studying human disease mechanisms were based on animals and heterologous expression systems which not reliable recapitulate disease phenotypes occurring in humans (Inoue and Yamanaka, 2011). Using iPSCs to model human diseases is based on ability to generate patient-specific pluripotent stem cells which contain specific disease-causing gene mutations in natural genetic environment (Inoue and Yamanaka, 2011). Disease-specific cells are produced from patient-specific stem cells by differentiating them into cell type affected in the disease allowing *in vitro* examination of disease mechanisms and phenotypic features. Especially iPSCs are great cell source for generating human cell types that are not otherwise available, and therefore many neurological and cardiological diseases have been modelled with iPSC-derived disease-specific cells (Inoue and Yamanaka, 2011).

In addition to *in vitro* applications, clinical potential of iPSCs in the field of regenerative medicine for repairing tissue damages has been evaluated due to the possibility to produce genetically identical cells with a patient (Laflamme et al., 2007; Zwi et al., 2009; Yoshida and Yamanaka, 2011). However, several concerns have been related to their clinical use. Firstly, although many non-viral delivery methods for transducing exogenous reprogramming factors have been developed, their efficiencies do not reach reprogramming efficiencies of viral delivery methods (Zwi et al., 2009). Increased risk of tumorigenesis due to integrated viral genome into host cell genome and possible reactivation of exogenous oncogenic c-Myc have been associated with the use of viral transduction methods for generating iPSCs. Secondly, differentiation protocols produce commonly heterogeneous cell population containing variable maturities and phenotypic features (Zwi et al., 2009). Incomplete and variable differentiation is suggested to be caused by epigenetic memory, indicating that iPSCs contain

DNA methylation patterns related to their somatic cell origin (Kim et al., 2010). Thus, iPSCs differentiate rather into their original lineage than into other lineages. Integrated viral genome and expression of unsilenced transgene also affect differentiation capacities of iPSCs (Yu et al., 2007; Zhang et al., 2009). Thirdly, heterogeneity of iPSCs causes variable growth and differentiation potentials among the cell population and reduces similarities between iPSCs and ESCs, resulting in their limited clinical potential (Narsinh et al., 2011). Nevertheless, iPSCs provide a remarkable research tool for examining disease phenotypes and mechanisms, discovering and testing new therapeutics and evaluating their efficacies in disease treatments (Inoue and Yamanaka, 2011; Moretti et al., 2013).

2.3.1. Cardiac differentiation of induced pluripotent stem cells

To create reliable *in vitro* disease models, efficient and robust protocols for differentiating induced pluripotent stem cells into cell type of interest have to be existed. There are three main methods used for differentiating iPSCs into functional cardiomyocytes in *in vitro* conditions: embryonic body (EB) differentiation, monolayer culturing and inductive co-culturing (Yoshida and Yamanaka, 2011; Mummery et al., 2012). The first attempts to generate cardiomyocytes from human iPSCs were performed by EB differentiation protocol that forms contracting embryonic bodies which express cardiac specific genes and proteins, have specific electrophysiological properties and react to β-adrenergic stimulation by increasing contraction rate (Zhang et al., 2009; Zwi et al., 2009). However, the amount of contracting EBs achieved by this differentiation protocol is not more than 10 % (Zhang et al., 2009), indicating that efficiency to produce functional cardiomyocytes is relatively poor. For that reason, direct differentiation protocols were developed to generate iPSC-derived cardiomyocytes (Mummery et al., 2012). Monolayer culturing of iPSCs enables effective administration of growth factors, such as activin A and BMP4, required for generating functional cardiomyocytes, and permits that their effects are targeted directly at differentiable stem cells (Laflamme et al., 2007; Zhang et al., 2012). Therefore, cardiac differentiation in the monolayer cultures is significantly more effective than in the EBs and produced cardiomyocytes are related to higher purity than can be isolated from EBs (Zhang et al., 2012). The other direct differentiation protocol is performed by co-culturing iPSCs with mouse visceral endoderm-like cells (END-2) which are able to induce differentiation of iPSCs into mesoderm-derived cardiac precursor cells, as known to occur during *in vivo* embryonic development (Mummery et al., 2003; Pekkanen-Mattila et al., 2009). This inductive co-

culture protocol is generally used to confirm cardiac differentiation capacity of iPSCs because it allows rapid production of functional cardiomyocytes (Mummery et al., 2012).

The *in vitro* cardiac differentiation of iPSCs mimics naturally occurring embryonic development of the human heart, known as cardiogenesis (Mummery et al., 2012). The differentiation process contains multiple steps that are regulated by various signaling pathways and growth factors (Moretti et al., 2013) which are represented in details in the figure 4. Bone morphogenetic proteins (BMPs), wingless/INT proteins (WNTs), fibroblast growth factors (FGFs), transforming growth factor β1 (TGF-β1) and activin A are major factors to regulate signaling pathways during cardiac development resulting in generation of multipotent cardiovascular progenitor cells having capacity to differentiate into cardiomyocytes, smooth muscle cells and vascular endothelial cells (Takahashi et al., 2007; Mummery et al., 2012; Moretti et al., 2013). During *in vitro* cardiac differentiation of iPSCs, sequential and accurate administration of growth factors by following their naturally occurring order allows efficient cardiomyocyte generation. Administration of activin A induces development of mesodermal progenitors which further differentiate into functional cardiomyocytes by adding BMP4 and bFGF (Zhang et al., 2012). Developmental stages within cardiac differentiation are characterized by immunocytochemical staining specific markers expressed by cells in different stages (figure 4.) (Mummery et al., 2012; Moretti et al., 2013).

In addition that cardiomyocytes are characterized by immunostaining cardiac structural proteins described in figure 4., their functionality has to be evaluated. Functional cardiomyocytes are able to contract spontaneously that can be observed as beating clusters in cell cultures. Their electrophysiological properties are detected and measured by using multielectrode array (MEA) (Zwi et al., 2009) or patch-clamp technology (Mummery et al., 2012). MEA is used for analyzing multicellular electrical activity (Egashira et al., 2012; Mummery et al., 2012) and contraction capacity (Zhang et al., 2009) from a beating cell cluster formed by cardiomyocytes by measuring field potential duration that can be used for calculating duration of QT interval (Matsa et al., 2011). Action potential development and duration can be evaluated with patch-clamp technology by determining ion conductance of

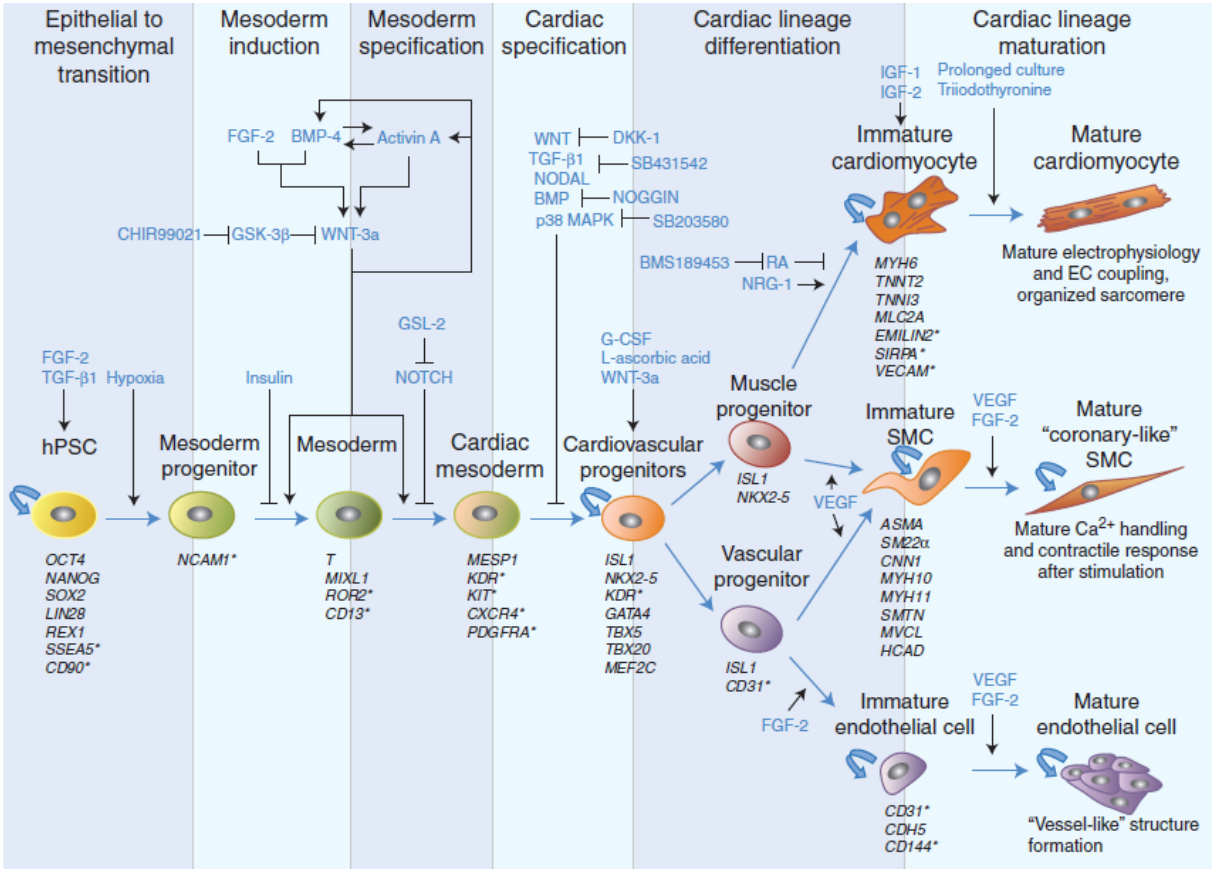

Figure 4. Cardiac differentiation of human induced pluripotent stem cells. Signaling pathways and growth factors (represented with blue) involve in progression of cardiac differentiation by either activating or inhibiting it. Specific markers expressed by cells in different developmental stages are described below the cell figures. Those could be used for characterizing distinct cells within developmental stages by immunocytochemical staining. The figure was modified from the origin Moretti et al., 2013.

cardiac ion channels within a single cardiomyocyte (Matsa et al., 2011; Mummery et al., 2012). Therefore, it is extremely useful for studying arrhythmic mechanisms caused by ion channel mutations or pharmaceuticals. Moreover, isoproterenol treatment is used to evaluate response of cardiomyocytes to β-adrenergic stimulation. Isoproterenol is an agonist for β-adrenoreceptor (Matsa et al., 2011) and therefore its administration into cardiomyocytes accelerates contraction rate and shortens APD (Zhang et al., 2009; Zwi et al., 2009). In LQTS-specific cardiomyocytes, isoproterenol commonly induces development of arrhythmic events and EADs (Egashira et al., 2012) and that is why it is generally used for reproducing arrhythmias, particularly TdPs, occurring in LQTS.

2.3.1.1. Modelling of long QT syndrome with disease-specific iPSCs

Human long QT syndrome has been attempted to recapitulate in many mouse models, but significant differences in electrophysiological properties between humans and mice have led to unsuccessful disease modeling. Although many similarities in ion channel structures have been detected, mice have 10-times faster heart rate than humans have, resulting in differences in ECGs and action potentials between the species (Salama and London, 2007). Furthermore, recapitulating human arrhythmic phenotypes of LQT1 and LQT2 subtypes by mouse models has emerged to be remarkably challenging due to the functional differences in cardiac K^+ ion channels (Salama and London, 2007). In contrast, zebra fish model for human LQT2 succeeded to recapitulate specific disease phenotype, including prolonged APD and QT interval and reduced I_{Kr} current in HERG channels (Arnaout et al., 2007). In addition, many heterologous expression systems have been used to study disease mechanisms of LQTS, but the lack of appropriate cardiac environment and channel-associating molecules have hampered reproduction of disease phenotypes (Medeiros-Domingo et al., 2007).

Several long QT syndrome models derived from disease-specific iPSCs have successfully reproduced specific LQTS-related disease phenotypes. Human LQTS models for LQT1 (Moretti et al., 2010; Egashira et al., 2012) and LQT2 (Itzhaki et al., 2011; Matsa et al., 2011; Lahti et al., 2012) subtypes have been characterized with typical electrophysiological features, such as prolonged APD caused by delayed repolarization phase and decreased amplitudes of K^+ ion currents, within iPSC-derived cardiomyocytes. Most of LQTS-specific cardiomyocytes used for disease modelling have been generated from patients who have experienced cardiac events during their lifetime (Itzhaki et al., 2011; Matsa et al., 2011; Egashira et al., 2012), but Lahti et al. (2012) succeeded to recapitulate LQT2-related disease phenotype from cardiomyocytes generated from asymptomatic patient with diagnosed HERG-FinB mutation, one of the four Finnish founder mutations. These findings indicate that LQTS models with specific phenotypic features can be generated from iPSC-derived cardiomyocytes of patient without manifested cardiac events (Lahti et al., 2012). Such disease models can be used to investigate cellular mechanisms that affect development of cardiac events among LQTS patients by comparing them with disease models generated from symptomatic mutation carriers. Long QT syndrome is an ideal disease to be modelled with iPSC-derived cardiomyocytes due to that underlying genetic cause and specific phenotypic features are mostly solved (Moretti et al., 2013). Thus, these LQTS disease models offer a tool for

studying more specific, relatively unknown, features. For example, they permit investigation of genetic and non-genetic factors that may cause phenotypic variation within LQTS patients (Lahti et al., 2012). However, current cardiac differentiation protocols commonly generate heterogeneous and poorly maturated cardiomyocyte population with phenotypic characteristics for all atrial, ventricular and nodal cells leading to reduced reliability of their usage for cardiac disease modelling (Zhang et al., 2012; Moretti et al., 2013).

In vitro LQTS disease models are perfect platforms to test and discover novel pharmaceuticals. Nowadays, main reasons for failed preclinical and clinical studies during drug development are cardiotoxicity, hepatotoxicity or neurotoxicity of tested medicines due to that these toxic effects can remain to be undetected in animal model studies performed during drug testing, and therefore risk of severe side effects is increasing (Inoue and Yamanaka, 2011). LQTS disease models can be utilized for predicting possible cardiotoxic effects. In addition, drug efficiency and required drug dosage to improve disease phenotypic features, such as shortening APD or preventing development of EADs, can be evaluated from LQTS models (Itzhaki et al., 2011). Due to the drug-induced form of LQTS caused by inhibited function of HERG ion channels, it is significantly important to identify drugs which have QT interval prolonging effects and may cause arrhythmic events (Itzhaki et al., 2011; Matsa et al., 2011; Egashira et al., 2012; Lahti et al., 2012). For their identification, LQTS models provide a useful detection system due to that their arrhythmogenic susceptibilities are already high.

2.4. Cell characterization with quantitative real-time PCR

Quantitative real-time PCR (qPCR) enables amplification of target gene by polymerase chain reaction (PCR) simultaneously with detection and quantification of amplifying PCR products (Heid et al., 1996; Arya et al., 2005). By using qPCR, pieces of genomic DNA can be detected using specific markers that allow evaluating of gene expression of interest. Thus, it is extremely useful method for cell and cell line characterization. Accurate and appropriate quantification is based on carefully designed primers and probes which permit amplification and detection of desired gene target, respectively. The qPCR system contains sequence detector which measures continuously fluorescent emissions occurring during PCR amplification (Heid et al., 1996). The detectable fluorescent emissions are resulted from fluorescent probes which have bound with amplifying targets. Mostly probes are labelled with

fluorescent dyes that develop fluorescence signals when cleaved from probe fragments (Heid et al., 1996). In addition, detection systems based on DNA-binding dyes, such as SYBR® Green 1, are used to quantify target expression during PCR amplification (Arya et al., 2005). DNA-binding dyes bind with all double-stranded DNA that is present in PCR reaction leading to increased risk of nonspecific detection. In contrast, fluorescent probes hybridize complementary with target sequence that increases specificity and reliability of detection of amplifying targets (Arya et al., 2005). Detection mechanisms of fluorescent probes are discussed in details in the next section, concentrating on chemistry of TaqMan® fluorescent probes.

Few parameters are essential to be familiar when PCR amplification data is analyzed. The amplification plot contains threshold level that is chosen according to baseline level, meaning the level in which detection capacity of qPCR system to observe fluorescence signals initiates (Arya et al., 2005). The threshold cycle or Ct value indicates the PCR cycle number in which fluorescence signal becomes distinguishable from the background fluorescence, and therefore, it describes the cycle number initiating detection of target during qPCR analysis. Ct values are directly comparative with initial target template concentrations (Heid et al., 1996; Arya et al., 2005). High initial concentration of target results in lower Ct values due to that there is higher amount of templates to be bound by probes, leading to earlier development and detection of fluorescence signals.

There are two main methods to evaluate qPCR results: standard curve and relative quantification (Livak et al., 2001; Arya et al., 2005). Standard curve method is based on generated standard samples containing known DNA concentrations by serially diluting them (Arya et al., 2005). Therefore, standard curve can be used for determining DNA concentrations of unknown samples by using their qPCR-measured Ct values. The other method is a relative quantification that enables quantification of target gene expression by normalizing the expression with endogenous housekeeping gene's expression (Livak et al., 2001; Arya et al., 2005). The used equation in that method is $2^{-\Delta\Delta Ct}$, where $\Delta\Delta Ct = \Delta Ct$ (sample) - ΔCt (control), and ΔCt = Ct (target gene) - Ct (housekeeping gene) (Livak et al., 2001). Appropriate housekeeping gene, which can be selected for normalization, has equal PCR amplification efficiency than target gene has and has constant expression levels in

different tissues (Arya et al., 2005). Selection of quantification method is dependent on the way that target gene expression is desired to be determine. The standard curve method permits absolute gene expression determinations; whereas the $2^{-\Delta\Delta Ct}$ method is more useful if target gene expression is determined as fold changes by comparing with expression of control gene (Livak et al., 2001).

2.4.1. TaqMan® Assays

TaqMan® Assays used in qPCR analysis provide allele-specific detection and quantification of amplified DNA samples. The main function of TaqMan® Assay during PCR reaction is represented in the figure 5. They contain forward and reverse primers which initiate amplification of target sequence resulted in polymerization of new complementary DNA strands. In addition, TaqMan® Assays contain specific probes designed to bind with specific genomic site of target sequence between primer binding sites and they are responsible for detection of amplifying target by qPCR system. Probe's 5'-end is labelled with reporter dye or fluorophore which function is prevented by 3'-end labelled quencher dye before PCR reaction (Arya et al., 2005). According to manufacturer's protocol for TaqMan® Universal PCR Master Mix (Applied Biosystems, Life Technologies Ltd.), AmpliTaq Gold® DNA polymerase performs polymerization of target sequence initiating from primers. The enzyme has 5'-3' nuclease activity causing degradation of bound probe when polymerizing strand reaches the probe. Therefore, fluorophore releases from the probe and it is not any longer be prevented by quencher dye, leading to occurrence of fluorescence signal. The qPCR system detects and measures fluorescence signal intensities that are increasing simultaneously when the amounts of amplified PCR products are increasing (Arya et al., 2005), and forms an amplification plot for each analyzed DNA sample according to its increased fluorescence intensity during PCR cycles.

TaqMan® Assays enable detection of allelic expression differences within heterozygous DNA samples. For example, they can be used for detecting expression differences between wild type and mutant alleles of certain gene. In order to examine allelic expression differences, TaqMan® Assays containing two different probes labelled with different fluorophores are used. Therefore, they generate different fluorescence signals during PCR reaction permitting detection of distinct allelic expressions. The probes are designed to hybridize with genomic sites where single nucleotide polymorphism (SNP) or mutation

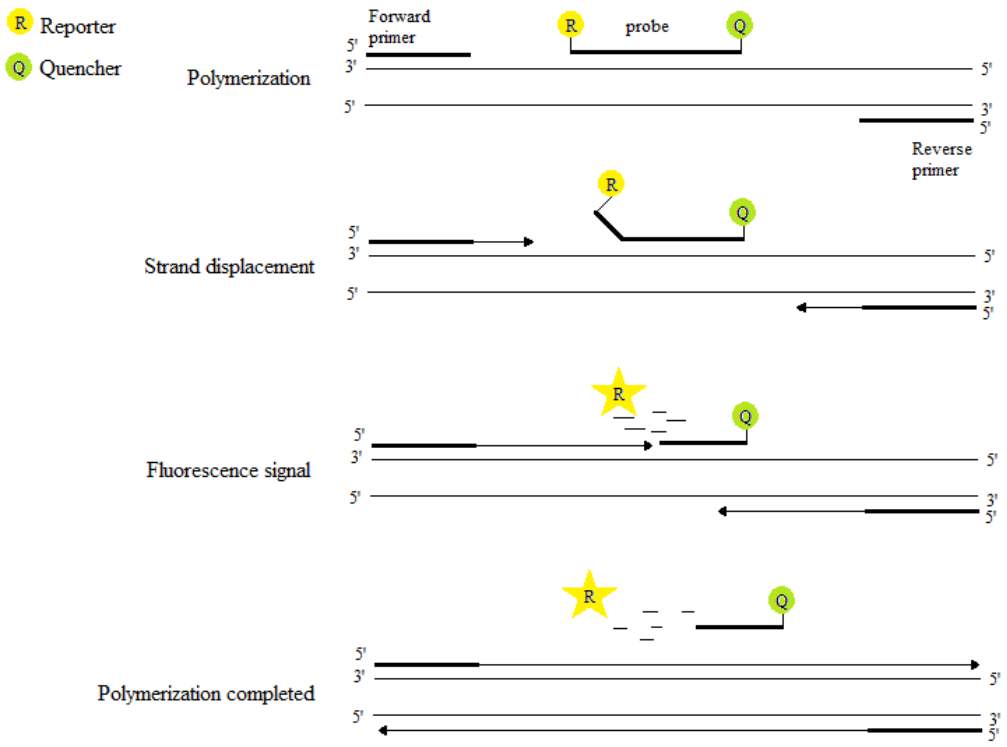

Figure 5. Function of TaqMan® Assays during PCR reaction. AmpliTaq Gold® DNA polymerase initiates polymerization of complementary DNA strand for target sequence from bound primers. Progressing polymerization displaces hybridized probe causing release of fluorophore and occurrence of fluorescence signal that is detected by qPCR system.

locates in mutant allele and corresponding site of the wild type allele. The qPCR system creates an allelic discrimination plot according to the measured fluorescence signal intensities from both probes that are described separately by y-axis and x-axis. If the qPCR system detects only one fluorescence signal, the DNA sample contains homozygote alleles, indicating either two wild type alleles or two mutant alleles depending on detected fluorophore signal. But if it measures fluorescence signals from both fluorophores, the DNA sample is heterozygous and contains both alleles. The proportions of detected fluorescence signals are described on the allelic discrimination plot allowing investigation of allelic expression differences within heterozygote sample.

2.4.2. Determination of allelic expression variation with quantitative real-time PCR

Variation in allelic expression is common among human genes between individuals and therefore it may be a genetic factor promoting disease development and causing phenotypic variation among humans (Lo et al., 2003; Buckland, 2004). Several familiar gene expression

variations occur in human genomes, such as X chromosome inactivation and identified imprinted genes that lead to expression of only one allele (Lo et al., 2003), and thereby may cause variation among mutation carriers with differently expressed alleles (Saenen and Vrints, 2008). In addition, many other human genes have shown differences in allelic expression that are suggested to be caused by gene transcription regulation, such as cis-acting elements or epigenetic modifications (Buckland, 2004), resulting in higher expression levels of other allele. Especially, variations in promoter regions or non-coding regions alter transcription rates due to defective binding of transcription factors or transcription regulation leading to variable expressions of alleles (Chen et al., 2008; Shen et al., 2011). However, many regulatory regions are mostly unidentified that have complicated determination of allelic imbalance effects for phenotypic features. Many methods for study variable allele-specific expression and quantify mRNA levels transcribed from both alleles have been developed, such as allele-specific microarray and single nucleotide primer extension (Buckland, 2004).

There are two main procedures to determine allelic expression differences of certain gene by using standard curves. The first one uses homozygote genomic DNA (Lo et al., 2003) or cDNA (Chen et al., 2008; Shen et al., 2011) derived from two individuals to produce standard samples, whereas the second method generates plasmids containing wild type and mutant inserts which are mixed with appropriate ratios (Moretti et al., 2010). Chen et al. (2008) examined the influences of allelic imbalances of *BRCA1* and *BRCA2* genes for breast cancer development. Allele-specific expression analysis was performed by using cDNA ratios generated from homozygous lymphocytes with specific polymorphisms in *BRCA1* (BRCA1-c.4308T/T or BRCA1-c.4308C/C) or *BRCA2* (BRCA2-c.3396A/A or BRCA2-c.3396G/G) genes. The homozygote cDNA samples were mixed together with various ratios: 8:1, 4:1, 2:1, 1:1, 1:2, 1:4 and 1:8 in order to form allelic expression standard curves for *BRCA1* and *BRCA2*. Those standard curves were used to determine allelic imbalance of either BRCA1-c.4308T/C or BRCA2-c.3396A/G heterozygote cells. They noticed that allelic imbalance of those genes is associated with increased risk of breast cancer. The mRNA and protein expression levels can reduce as a result of allelic expression differences and that could lead to development of disease state (Chen et al., 2008). Shen et al. (2011) used the same method to evaluate the effects of allelic imbalance related to *BRCA1* and *BRCA2* genes for development of familial ovarian cancer. They confirmed that high allelic imbalance of *BRCA1* gene is significantly related to low mRNA expression levels and increased risk of familial ovarian

cancer. Therefore, allelic imbalance might be remarkable genetic factor to contribute disease development and phenotypic variations.

Plasmid-derived standard curve method for determining allelic imbalance was developed by Moretti et al. (2010). They generated two plasmids: one contained insert of genomic site of wild type allele and the other contained insert of corresponding mutant allele with specific LQT1-causing *KCNQ1* gene mutation. R190Q is a missense mutation locating in cytoplasmic loop between S2 and S3 segments of KCNQ1 α-subunit (Moretti et al., 2010). The mutational mechanism related to it is reduced transportation of mutated α-subunits to the cell membrane leading to decreased amount of functional I_{Ks}-conducting K^+ ion channels in dominantly negative manner. Wild type and mutant plasmids were mixed with similar ratios described by Chen et al. (2008) and standard curve was plotted $\log_2$(WT/MUT) vs. ΔCt values. Allelic expression differences of heterozygote patient-specific iPSC-derived cardiomyocytes were analyzed from standard curve. They observed that R190Q-mutated cardiomyocytes had equal expression of wild type and mutant alleles, and any mRNA or protein level differences were not detected between LQT1-specific and control cardiomyocytes.

2.4.3. Single-cell gene expression analysis by using quantitative real-time PCR

Interest toward single-cell technologies has increased during few decades in research field because they enable to examine and evaluate behavioral and functional differences between single cells within cell population (Kalisky et al., 2011). Those technologies identify heterogeneity by detecting and quantifying mRNA transcripts of target genes with fluorescent in situ hybridization, qPCR or microarray methods or ultimately sequencing whole genome in order to access genetic information cannot be examine with other methods (Kalisky et al., 2011; Ståhlberg et al., 2011). Functional cell-to-cell variations cannot be determined with cell population studies due to that individual cells have their own gene expression profile causing differences in mRNA and protein levels that affect to development of different cell fates (Peixoto et al., 2004; Bengtsson et al., 2008). It has also been observed that gene expression levels may differ significantly between studies performed at cell population or single cell levels, leading to suggestions that gene expression occurring in cell population is average of the expression occurring within individual cells (Peixoto et al., 2004; Fox et al., 2012). Cellular mechanisms that cause gene expression variation and heterogeneity among even

genetically and phenotypically identical cell population are highly unidentified (Glotzbach et al., 2011). Stochastic gene expression has been suggested to be a potential mechanism leading to variable expressions and transcription rates between individual cells (Elowitz et al., 2002; Raj et al., 2010). In addition, available transcriptionally active chromatin causes gene expression differences and it could be promoted by mutations in molecules regulating chromatin's conformational changes (Raj et al., 2010).

Because mRNA levels in individual cells are very low, multiple gene expression analysis has to perform in a single PCR reaction containing multiple primers for amplifying all target genes of interest (Taniguchi et al., 2009). Therefore, any competition between used primers at pre-amplification or amplification stages may induce unbalanced amplification of targets causing higher amplification of particular target mRNAs, while the other mRNAs are not amplified with the same rate and efficiency (Peixoto et al., 2004). Thus, possible primer competition has to be evaluated before qPCR analysis in order to achieve efficient and accurate single-cell multiplex gene expression analysis. To evaluate primer competition, pre-amplification is performed separately with single and pooled primers, and if these experiments produce similar Ct values during qPCR analyses, primers are not competitive (Ciriza et al., 2012). But if any competition is observed, gene expression analyses have to perform separately with divided single cell samples or other methods have to be used (Taniguchi et al., 2009). Pre-amplification is usually necessary to perform before qPCR analysis in order to increase the amount of target template and it can be performed by either selective amplifying specific mRNA targets or amplifying all mRNAs present in cells (Freeman et al., 1999). Additionally, it has been observed that current single-cell gene expression technologies determine effective gene expression from abundant mRNAs but their efficiencies are not sufficient to quantify expression of more rare mRNAs (Bengtsson et al., 2008).

Before quantification of gene expression levels, single cells are isolated from heterogeneous population by using appropriate techniques. Single cells can be collected by manually isolating cells of interest with micropipette (Freeman et al., 1999), or using more technical methods, such as laser capture microdissection (Fox et al., 2012) or fluorescence activated cell sorting (Glotzbach et al., 2011; Narsinh et al., 2011). Single cell isolation is usually

followed by cell lysis in many technologies (Fox et al., 2012) due to that using cell lysis can be avoided loss of mRNAs associated with basic RNA purification methods (Bengtsson et al., 2008). Techniques developed for characterizing single-cell gene expression are commonly based on the use of basic qPCR or microfluidic PCR (Fox et al., 2012). When comparing to basic qPCR analysis, the significant advantage of microfluidic PCR analysis is the capacity to perform thousands of single cell assays parallel in tiny reaction volumes (White et al., 2011) and therefore, it enables single-cell gene expression analysis in high throughput manner. Chip-based (Glotzbach et al., 2011; White et al., 2011) and droplet-based (Brouzes et al., 2009) approaches are used in microfluidic PCR analysis. Both methods permit gene expression analysis in integrated and automatic processes, indicating that total workflow initiating from single cell isolation and finishing to detection of target gene expression is performed sequentially and simultaneously in the same device.

Single-cell gene expression analysis permits characterization of single cells among population based on their specific gene expression profiles that could be earlier studied only at cell population level (Peixoto et al., 2004; Narsinh et al., 2011). Multiple population heterogeneity determinations have been performed by using qPCR-based methods. For example, significant gene expression heterogeneity has been revealed to occur within induced pluripotent stem cells and iPSC-derived differentiated cell types that affect their pluripotencies and differentiation capacities (Narsinh et al., 2011). The population heterogeneity studies may provide essential new knowledge about functional roles of individual cells in development or progression of disease state (Fox et al., 2012). Single-cell based analysis has been used in clinical diagnostic tests, especially in cancer (Ståhlberg et al., 2011) and stem cell (White et al., 2011) researches due to that heterogeneity within these cell populations are commonly high. In tumor diagnostics, the single-cell gene expression analysis permits characterization of specific cell types, such as cancer stem cells and circulating tumor cells, within tumor cell population and therefore facilitates their identification and enhances the treatment decisions (Ståhlberg et al., 2011). However, efficiencies of many gene expression analysis technologies are nowadays still limited to characterize cells on the cell population level, although the development of single-cell based technologies has increased enormously.

3. Aim of study

The aim of this study was to evaluate specific genetic features occurring within LQTS-specific cardiomyocytes by using quantitative real-time polymerase chain reaction. This study consisted of three different experiments in which qPCR was used to detect either amplification of cardiac ion channel genes or typical structural genes or their allelic expression differences in order to characterize iPSC-derived LQTS-specific cardiomyocytes contained predominating disease-causing mutations in Finland.

In the first experiment was evaluated capacity of cell lysis -based genotyping method to characterize cardiac cell lines with appropriate detection specificity. The purpose was to solve if the method could be used for facilitated genotyping of disease-specific cardiac cell lines in an everyday routine manner. In the second experiment, the effect of allelic expression variation for variable phenotypic features associated with LQTS was evaluated by using plasmid-derived standard curve method and qPCR (Moretti et al., 2010). Allelic imbalance determinations were performed for Finnish founder mutation specific cardiomyocytes and therefore the study was also allowed investigations of genetic mechanisms which may have enhanced enrichment of those mutations among Finnish population and lead to development of milder phenotypic effects suggested to be related to founder mutations (Piippo et al., 2001).

The intend of the final experiment was to led cardiomyocyte characterization from cell population level to the single cell level by using specific qPCR-based procedure for evaluating expressions of basic structural protein within low amount cell samples and multiple cell samples. Single-cell gene expression analysis methods enable to examine cell population heterogeneity causing variations for functions and behaviors of individual cells (Kalisky et al., 2011). Therefore, this single-cell qPCR analysis was expected to reveal whether the method could be able to characterize more specific cardiac gene expressions in the future.

4. Materials and methods

4.1. Disease-specific induced pluripotent stem cells

Disease-specific iPSCs were generated from fibroblasts isolated from skin biopsies of patients who carry LQTS-related Finnish founder mutations (KCNQ1-FinA, KCNQ1-FinB, HERG-FinA or HERG-FinB). Isolation and use of patient-specific cells in researches were approved by the ethical committee of Pirkanmaa Hospital District (R07080). Fibroblast culturing conditions in which isolated fibroblasts were maintained have been described previously by Lahti et al. (2012).

Reprogramming of patient-specific fibroblasts was performed with iPSC technology developed by Takahashi et al. (2007). Four transcription factors, Oct4, Sox2, Klf4 and c-Myc, were delivered into fibroblasts using first lentiviral vectors followed by transduction with retro- or Sendai-viruses (Lahti et al., 2012). The plasmids, cells and reagents used in reprogramming processes have been represented previously (Lahti et al., 2012). In this study, six LQTS-specific iPSCs lines and three iPSCs lines derived from healthy individuals have been used (table 2.). Their pluripotency were confirmed by immunocytochemical staining the protein expressions of pluripotency-related genes, and their differentiation capacity to form EBs *in vitro* and teratomas *in vivo* which contain derivatives from all three germ layers was verified as has been described by Lahti et al. (2012).

4.1.1. Cardiac differentiation of iPSCs

Cardiac differentiation of patient-specific iPSCs was performed by co-culturing them with END-2 cells, as has been described previously (Mummery et al., 2003; Pekkanen-Mattila et al., 2009). Co-culture with END-2 cells induced differentiation of iPSCs into cardiomyocytes which formed beating clusters in the cell culture plates. Their differentiation was verified by immunocytochemical staining the protein expressions of cardiac specific genes and detecting specific electrophysiological features (Lahti et al., 2012). LQTS-specific cardiac cell lines and wild type cell lines that were used in this study are represented in the table 2.

4.2. RNA isolation and cDNA transcription

Beating areas containing functional cardiomyocytes were cut by using scalpel under a microscope and the areas were transferred into Lysis Buffer R1 with β-mercaptoethanol for RNA isolation. In this study, NucleoSpin® RNA II Kit (Macherey-Nagel GmbH & Co.,

Table 2. iPSC-derived cardiac cell lines used in this study. Letter "s" in the end of names UTA.04311.WTs and UTA.04511.WTs indicates that those cardiomyocyte lines have been differentiated from iPSC lines transduced by Sendai-virus. Otherwise, retroviral transduction for reprogramming has been used.

Cardiac cell line	Disease	Mutation
UTA.00208.LQT1	Long QT syndrome type 1	KCNQ1-FinA (G589D)
UTA.02201.LQT1	Long QT syndrome type 1	KCNQ1-FinA (G589D)
UTA.00118.LQT1	Long QT syndrome type 1	KCNQ1-FinB (IVS7-2A>G)
UTA.03412.LQT2	Long QT syndrome type 2	HERG-FinA (L552S)
UTA.03810.LQT2	Long QT syndrome type 2	HERG-FinA (L552S)
UTA.00525.LQT2	Long QT syndrome type 2	HERG-FinB (R176W)
UTA.04602.WT	None	None
UTA.04311.WTs	None	None
UTA.04511.WTs	None	None

Düren, Germany) was used for total RNA isolations by following purification protocol described by manufacturer. The concentrations of isolated RNA samples were measured with NanoDrop 1000 spectrophotometer (Thermo Scientific, Wilmington, DE, USA). Then, isolated RNAs were reverse transcribed to complementary DNAs (cDNA) by using High Capacity cDNA Reverse Transcription Kit (Applied Biosystems, Life Technologies Ltd., Carlsbad, CA, USA). The cDNA transcription was occurred according to manufacturer's protocol, and used reverse transcription master mix contained 2 µl 10x RT Buffer (1.0 ml), 0,8 µl 25x dNTP Mix (100 mM), 2µl 10x RT Random Primers (1,0 ml), 1µl MultiScribe™ Reverse Transcriptase (50 U/µl), 0,5 µl RNase Inhibitor (100 µl) and 3,7 µl DNase-free water. For every cDNA transcription, 10 µl RNA was added into 10 µl reverse transcription master mix. Thermal cycler used for cDNA transcription was Eppendorf MasterCycler EP Gradient S (Eppendorf, Hamburg, Germany) and used RT-PCR program was 10 min 25°C, 120 min 37°C and 5 min 85°C.

4.3. Cell line characterization

Commercially available TaqMan® Sample-to-SNP™ Kit (Applied Biosystems, Life Technologies Ltd., Carlsbad, CA, USA) was used for performing cell line characterization of UTA.00208.LQT1 (heterozygous for KCNQ1-FinA mutation), UTA.04311.WTs and UTA.04511.WTs cell lines. Characterized cell samples were made by scratching the bottom of the cell culture plate with pipette's tip and transferring detached cells into the tubes containing culture media. Cell samples were lysed according to the protocol's instruction for cell culture suspension. PCR reaction master mix contained 10 µl 2x TaqMan® GTXpress Master Mix, 0,5 µl 40x Custom TaqMan® SNP Genotyping Assay and 5,5 µl DNase-free water. Used Custom TaqMan® SNP Genotyping Assay (Applied Biosystems, Life

Technologies Ltd., Carlsbad, CA, USA) contained primers and probes which were designed to amplify and detect KCNQ1-FinA mutated alleles and corresponding wild type (WT) alleles from cardiomyocyte samples. The Custom TaqMan® SNP Genotyping Assay was obtained from Assay service (Life Technologies Ltd.) and its assay ID and sequences of primers and probes are represented in the table 4. PCR reaction volume was 20 µl consisted of 16 µl PCR reaction master mix and 4 µl cell lysate. Each cell sample was analyzed as triplicates. The qPCR analysis was performed with 7300 Real-Time PCR System (Applied Biosystems, Life Technologies Ltd.) and thermal cycler condition at amplification phase was 2 min at 50°C, 10 min at 95°C, and 40 cycles of 15 sec at 95°C and 1 min at 60°C. Before amplification, pre-run was performed to measure background fluorescence, and after amplification, post-run was performed to determine fluorescence signal intensities from plate wells contained analyzed cardiomyocyte samples. The 7300 System SDS software (version 1.4) created allelic discrimination plot according to measured fluorescence intensities that were stored into the PCR amplification data.

4.4. Generation of plasmids for allelic imbalance determination

To determine allelic imbalances of KCNQ1-FinA, KCNQ1-FinB, HERG-FinA and HERG-FinB mutations, wild type (WT) and mutant (MUT) plasmids were generated by inserting corresponding fragments of wild type allele and mutant allele of each mutation. WT plasmids were generated from cDNA sample of UTA.04602.WT cell line by amplifying genetic site of wild type alleles with specific primers designed for each mutation. Forward primers and reverse primers (table 3.) had restriction sites for BamHI (Thermo Fisher Scientific Inc., Waltham, MA, USA) and NotI (Thermo Fisher Scientific Inc.) enzymes, respectively. The sizes of the wild type inserts were 382 bp, 482 bp, 320 bp and 233 bp for KCNQ1-FinA, KCNQ1-FinB, HERG-FinA and HERG-FinB mutations, respectively. Wild type and mutant allele fragments were inserted into pBluescript SK+ plasmids (Addgene, Cambridge, MA, USA) which have also restriction sites for BamHI and NotI, and therefore proper ligations of amplified wild type and mutant alleles into plasmids were occurred.

Mutant plasmids for KCNQ1-FinA and KCNQ1-FinB were produced from heterozygous cDNA samples of UTA.00208.LQT1 and UTA.00118.LQT1 cell lines, respectively, by amplifying mutant alleles with specific primers (table 3.) in PCR reactions. After PCR amplification, heterozygous amplified cDNAs of KCNQ1-FinA and KCNQ1-FinB specific

cardiomyocytes were treated with KasI restriction enzyme (New England Biolabs, Ipswich, MA, USA) in order to digest WT alleles and remain mutated alleles. Mutant inserts were purified using agarose gel electrophoresis before their insertions into BamHI-NotI-site of pBluescript SK+ plasmids (Addgene). The mutant insert contained KCNQ1-FinA mutation was 382 bp long, and the mutant insert contained KCNQ1-FinB mutation was 512 bp long, indicating insertion of 30 bp as compared to wild type insert (482 bp). Mutant plasmids of HERG-FinA and HERG-FinB were generated from their WT plasmids by using QuikChange II Site-Directed Mutagenesis Kit (Agilent Technologies Inc., Santa Clara, CA, USA). Designed mutagenic primers containing desired *KCNH2* mutations are described in the table 3. Mutagenesis of WT plasmids were induced according to manufacturer's instructions. All plasmid constructs were sequenced for verifying proper insertion of wild type and mutant fragments.

Table 3. The sequences of primers used in PCR amplification and QuikChange II Site-Directed Mutagenesis during plasmid generation for allelic imbalance determination. Forward and reverse primers contained BamHI and NotI restriction sites, respectively. Mutagenic primers were used only for HERG plasmids to produce specific mutations (HERG-FinA or HERG-FinB) into wild type plasmids.

Target	PCR amplification: forward primer with BamHI restriction site (5'-3')	PCR amplification: reverse primer with NotI restriction site (5'-3')	Mutagenesis: sense primer (5'-3')	Mutagenesis: antisense primer (5'-3')
KCNQ1-FinA	GCGGGATCCGAAATTCCAGCAAGCGCGGA	GCCGCGGCCGCCAGGAAGAGCTCAGGGTCGA		
KCNQ1-FinB	GCGGGATCCTTTGCCATCTCCTTCTTTGC	GCGGCGGCCGCGTCTCCCCTTCCAGGTCC		
HERG-FinA	GCGGGATCCCTGAAGACTGCGCGGCTGCT	GCGGCGGCCGCGGCCGACACGTTGCCGAAGA	GCGGCCGTGCTGTTCTCGCTCATGTGCA	TGCACATGAGCGAGAACAGCACGGCCGC
HERG-FinB	GCGGGATCCGGCTCATGACACCAACCACCGG	GCGGCGGCCGCCCATGGCTGTCACTTCGTCCAG	CGCTGACGGCCTGGGAGTCGTCG	CGACGACTCCCAGGCCGTCAGCG

Generated WT and MUT plasmids were transferred to H7 bacteria cells to grow and multiply over a night at 37 °C. The plasmids were purified from bacteria cell cultures by using NucleoBond® Xtra Midi (Macherey-Nagel GmbH & Co., Düren, Germany) method and purifications were performed by slightly modifying manufacturer's protocol. Structural integrities of purified plasmids were confirmed by running samples on 1% agarose gel.

Plasmid purities and DNA concentrations were measured with NanoDrop 1000 spectrophotometer (Thermo Scientific).

4.5. Allelic imbalance determination

Allelic imbalance determinations were performed for KCNQ1-FinA, KCNQ1-FinB, HERG-FinA and HERG-FinB mutations by utilizing the capacity of qPCR to detect allelic expression differences between wild type and mutant alleles of heterozygous disease-specific cardiomyocytes. Allelic imbalances were determined by plasmid-derived standard curve method that has been described previously by Moretti et al. (2010). WT and MUT plasmids were mixed with various ratios: 1:0, 8:1, 4:1, 2:1, 1:1, 1:2, 1:4, 1:8, and 0:1, respectively, in order to form the standard curves. Each plasmid ratio contained 1 ng/µl total plasmid DNA. The amounts of wild type and mutant plasmids were calculated according to their plasmid DNA concentrations and their proportions in each final plasmid ratio.

Plasmid-derived standard curves were used to evaluate allelic expression differences occurring in heterozygous LQTS-mutated cardiomyocytes. Therefore, cDNA samples of LQTS-specific cardiomyocytes were produced to be analysed simultaneously together with plasmid mixes by qPCR system. The cDNA transcription was occurred as have been described above. For detecting expression differences between WT and mutant alleles and plasmids, Custom TaqMan® SNP Genotyping Assays (Applied Biosystems, Life Technologies Ltd., Carlsbad, CA, USA) were used due to that they contain different probes for wild type and mutant targets labelled with different fluorophores (VIC-labelled probe for WT and FAM-labelled probe for MUT). Custom TaqMan® SNP Genotyping Assays were obtained from Assay service (Life Technologies Ltd.) and the sequences of primers and probes are represented in the table 4. PCR reaction mix contained 7,5 µl 2x TaqMan® Universal PCR Master Mix, 0,375 µl Custom TaqMan® SNP Genotyping Assay, and 2,125 µl DNase-free water. Each PCR reaction consisted of 12 µl PCR reaction mix and 3µl cDNA or plasmid DNA. Plasmid mixes and cardiomyocyte cDNA samples were analysed as triplicates. The qPCR analyses were performed with 7300 Real-Time PCR System (Applied Biosystems, Life Technologies Ltd.) and similar thermal cycler condition was used at amplification phase that described above. In addition, pre-run and post-run were performed at the beginning and at the end of the qPCR analyses, respectively. The used quantification method was absolute quantification enabling formation of allelic discrimination.

Table 4**.** Custom TaqMan® SNP Genotyping Assays used in allelic imbalance determinations of LQTS-causing mutations. Probes labelled with VIC fluorophore bind with the sites of the wild type alleles within WT plasmids or cardiomyocyte samples, whereas probes with FAM fluorophore bind with the mutated sites of the mutant plasmids or mutated alleles of cardiomyocytes. Also Assay IDs from Assay service (Life Technologies Ltd.) for each marker have been described.

Target	Primer/probe	Sequence 5'-3'	Assay ID
KCNQ1-FinA	Forward primer Reverse primer Probe wild type_VIC Probe mutation_FAM	CCCCCATAGAAAAGAGCAAGGAT CTACCTTGTCTTCTACTCGGTTCAG CGATCGGCGCCCGC ACGATCGACGCCCGC	AHCS714
KCNQ1-FinB	Forward primer Reverse primer Probe wild type_VIC Probe mutation_FAM	GCTCGGGGTTTGCCCTGAAGG GGCAGCATAGCACCTCCA CTCATTCAGACCGC CGACCTCGGACCGC	AHGJ2KS
HERG-FinA	Forward primer Reverse primer Probe wild type_VIC Probe mutation_FAM	AGCTGGATCGCTACTCAGAGT GCGATGAGCGCAAAGGT CACATGAGCAAGAACA CACATGAGCGAGAACA	AH20Z2J
HERG-FinB	Forward primer Reverse primer Probe wild type_VIC Probe mutation_FAM	CCAAGACCTTCCGCCTGAA TCCACGTCCACCACCAC ACGACTCCCGGGCCGT CGACTCCCAGGCCGT	AH39X8R

4.5.1. Standard curve method for evaluating allelic imbalances

Allelic imbalances of LQTS-specific cardiomyocytes, containing one of the four Finnish founder mutations, were determined with plasmid-derived standard curves. The standard curves were plotted $\log_2$ of wild type/mutant ratios of plasmids [$\log_2$(WT/MUT)] versus corresponding ΔCt values (Moretti et al., 2010). The ΔCt values were defined by subtracting Ct value of wild type marker from Ct value of mutant marker (ΔCt = Ct (mutant) - Ct (wild type)). The Ct values were measured during PCR amplification by qPCR system (7300 Real-Time PCR System, Applied Biosystems, Life Technologies Ltd.) and stored into amplification data of 7300 System SDS software (version 1.4). Amplification data was exported to the Microsoft Excel (2010) for further processing and formatting standard curves.

In the plasmid-derived standard curves, ΔCt values for plasmid ratios are represented in statistical form of mean ± standard deviation (n=3). Equations and linear regressions (R^2 values) were evaluated for all standard curves by using Microsoft Excel (2010). The R^2 values were used to estimate linearities of standard curves. The $\log_2$(WT/MUT) values for disease-specific cDNA samples were calculated from the standard curves' equations by using their mean ΔCt values (n=3). The locations of LQTS-specific cardiomyocyte samples on the

standard curve were estimated according to calculated $\log_2$(WT/MUT) versus ΔCt values. Comparing location of specific cell samples with nearby plasmid ratios on the standard curve, allelic imbalances for each studied LQTS-related mutation were investigated.

4.6. Single-cell gene expression determination

Capacity of commercially available Single cell-to-CT™ Kit (Ambion®, Life Technologies Ltd., Carlsbad, CA, USA) to detect protein expression of essential structural gene, cardiac troponin T2 from cardiomyocytes was studied in this experiment. The Single cell-to-CT™ Kit is a technology based on qPCR's ability to quantify gene expression levels via measured mRNA levels, and it enable detection of gene expression within a single cell. Cardiac troponin T2 (*TNNT2*) was selected to be a target gene due to its abundant expression in cardiomyocytes. Therefore, its detection is more confident in single-cell gene expression analysis than cardiac genes having lower expression levels (Bengtsson et al., 2008). *RPLP0* was used as an endogenous reference gene in order to normalize *TNNT2* expression.

Cardiac cell line UTA.00208.LQT1 was dissociated into 48-well culture plate to intend that every well contain 1-10 beating cardiomyocytes, as manufacturer's protocol defined sample size to be. By using a microscope, well which had two beating UTA.00208.LQT1 cells were selected for cell lysis procedure. In addition, two samples having plenty of cardiomyocytes from UTA.04311.WTs cell line were used as controls in order to evaluate ability of the method to detect gene expression from samples with multiple cells and compare detected gene expression results between single cell level and cell population level. Wells that contained cells of interest were washed twice with phosphate buffered saline (PBS) in order to prevent disruption of culture media for cell lysis procedure. Cell lysis was performed according to manufacturer's protocol by adding Single Cell Lysis mix into the washed wells. Cell lysates were collected from the wells to the PCR tubes which were used for further procedures of the method.

Testing Single cell-to-CT™ Kit (Ambion®, Life Technologies Ltd.) was performed by following manufacturer's protocol and defined reaction mixes and thermal cycler conditions in reverse transcription, pre-amplification and qPCR amplification steps. To perform pre-amplification of cDNA samples transcribed from cell lysates, 20x TaqMan® Gene Expression

Assays (Applied Biosystems, Life Technologies Ltd., Carlsbad, CA, USA) of TNNT2 and RPLP0 were pooled at the final concentration of 0,2x. TaqMan® Gene Expression Assays were obtained from Assay service (Life Technologies Ltd.) with Assay IDs Hs00165960_m1 and Hs04189669_g1 for TNNT2 and RPLP0, respectively. Pre-amplified cDNA samples were diluted 1:20 with 1x TE Buffer (pH 8.0), and those diluted samples were analyzed by 7300 Real-Time PCR System (Applied Biosystems, Life Technologies Ltd.) in order to quantify expressions of TNNT2 and RPLP0 within used cardiomyocyte samples. Therefore, two different PCR reaction mixes were prepared, one contained 20x TaqMan® Gene Expression Assay of TNNT2 and the other contained 20x TaqMan® Gene Expression Assay of RPLP0. Cell samples (one from UTA.00208.LQT1 and two from UTA.04311.WTs cell lines) were analyzed as triplicates and both PCR reaction mixes were used for each sample. The qPCR analysis was performed in MicroAmp Optical 96-well reaction plate (Applied Biosystems, Life Technologies Ltd.) using 50 µl reaction volume consisted of 10 µl 1:20 diluted pre-amplified cDNA samples and 40 µl reaction mix. Relative quantitation (ddCt) method was used to detect TNNT2 target and RPLP0 endogenous control from cell samples.

5. Results

5.1. Cell line characterization

The allelic discrimination plot (figure 6.) describes the results from cardiac cell line characterization with cell lysis -based TaqMan® Sample-to-SNP™ Kit (Applied Biosystems, Life Technologies Ltd.). There are observable differences between analyzed LQT1-specific cell line samples (UTA.00208.LQT1) and WT cell line samples (UTA.04311.WTs and UTA.04511.WTs) in their locations on the allelic discrimination plot resulting from different allelic contents. The LQT1-specific cDNA samples located in the middle of the allelic discrimination plot (figure 6.), indicating allelic content of both mutated and wild type alleles. Analyzed cDNA samples produced from cardiac WT cell lines were homozygotes, indicating that they contained only wild type alleles. Therefore, increased fluorescence intensities were measured only from VIC-labelled probes within characterized WT samples during PCR amplification. Similar results were observed when multiple LQTS-specific, CPVT-specific and WT cell lines were characterized using specific markers for four Finnish founder mutations with TaqMan® Sample-to-SNP™ Kit (Applied Biosystems, Life Technologies Ltd.) (data not shown).

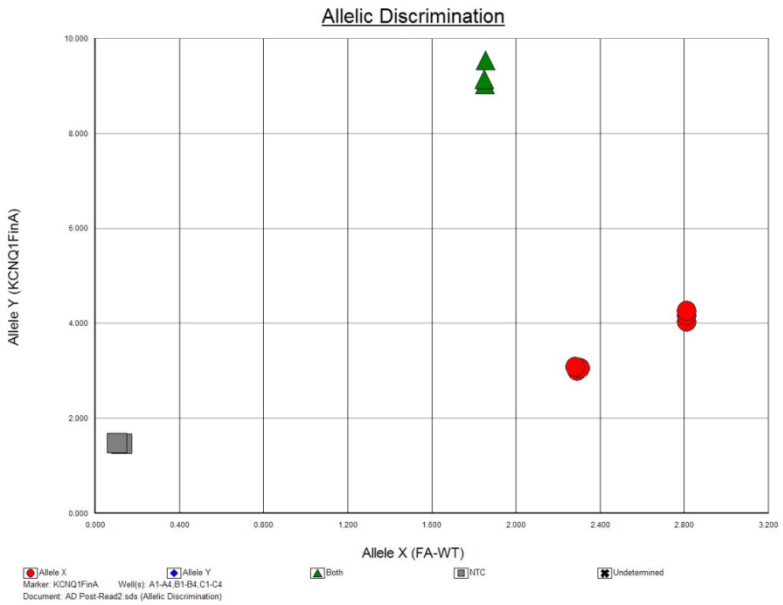

Figure 6. Allelic discrimination plot of characterized cardiac cell line samples. Samples from UTA.04311.WTs and UTA.04511.WTs lines are represented as red circles indicating homozygous wild type allelic contents. Heterozygote KCNQ1-FinA mutated cardiomyocytes (UTA.00208.LQT1) are represented as green triangles due to detected fluorescence signals from both probes included in used TaqMan® Assay. The cDNA samples were analyzed as triplicates. Sterile water was used as non-template control (NTC, grey squares) in analyses.

5.2. Allelic imbalance determination

Plasmid-derived standard curve method was used to determine allelic imbalances of LQTS-specific cardiomyocytes derived from induced pluripotent stem cells as have been previously described by Moretti et al. (2010). In this study, allelic imbalances were determined for LQTS-causing four Finnish founder mutations characterized in *KCNQ1* and *KCNH2* genes. Therefore, eight different plasmids containing mutant and wild type inserts for all determined mutations were generated. To form standard curve, WT and mutant plasmids were mixed with various ratios: 1:0, 8:1, 4:1, 2:1, 1:1, 1:2, 1:4, 1:8 and 0:1, respectively (Moretti et al., 2010). The plasmid ratios contained only WT (1:0) or MUT (0:1) plasmid were used as controls in order to confirm detection specificity of qPCR system during PCR amplification. They were not used to form standard curves due to undetermined detection of either wild type or mutant target amplification that prevents calculating ΔCt values. In addition, $\log_2$(WT/MUT) values cannot be calculated when the other plasmid content is lacking. Therefore, plasmid-derived standard curves were formed by plotting $\log_2$(WT/MUT) values versus ΔCt values defined for plasmid mixes 8:1, 4:1, 2:1, 1:1,1:2, 1:4 and 1:8.

5.2.1. KCNQ1-FinA and KCNQ1-FinB mutations

The cDNA samples used to determine allelic imbalance of KCNQ1-FinA specific cardiomyocytes were produced from cell lines UTA.02201.LQT1 and UTA.00208.LQT1 that have been generated from patient-specific iPSCs of two KCNQ1-FinA mutation carriers. To evaluate allelic imbalance of KCNQ1-FinB specific cardiomyocytes, cDNA samples were produced from cell line UTA.00118.LQT1 generated from patient-specific iPSCs of individual who carries KCNQ1-FinB mutation.

The plasmid mixes located on the allelic discrimination plots according to their plasmid ratio contents, as expected, in KCNQ1-FinA (figure 7A) and KCNQ1-FinB (figure 7C) specific analyses. In the allelic discrimination plot, the y-axis describes fluorescence intensity growth originated from FAM-labelled probes, whereas x-axis describes increase of fluorescence intensity detected from VIC-labelled probes. Therefore, plasmid mix contained only MUT plasmids (0:1) had the highest detected fluorescence intensity of FAM-labelled probes. Consistently, plasmid mix contained only WT plasmids (1:0) generated fluorescence signals from VIC-labelled probes. The other plasmid mixes (8:1, 4:1, 2:1, 1:1, 1:2, 1:4, and 1:8) were

arranged between them according to measured fluorescence intensities from both probes depending on WT and MUT plasmid proportions (figure 7A, 7C).

The allelic discrimination plot can be used for predicting allele-specific expression occurring in analyzed cardiomyocyte samples by comparing their locations with nearby plasmid mixes with known allelic contents. In the KCNQ1-FinA specific analysis, all mutant cDNA samples clustered between 1:1 and 2:1 (WT:MUT) plasmid mixes but few of them had slightly lower fluorescence intensities of FAM fluorophore as compared to nearby plasmid mixes (figure 7B). Relatively similar clustering was observed with KCNQ1-FinB specific cDNA samples within fluorescence intensity curve made by KCNQ1-FinB specific plasmid mixes (figure 7D). However, allelic discrimination plot is only rough method to confirm that heterozygote cardiomyocytes locate among heterozygote plasmid mixes, and therefore, it cannot be used directly for determining allelic expression variation of LQTS-mutated cardiomyocytes. For that reason, standard curves [$\log_2$(WT/MUT) vs. ΔCt] were formed for evaluating allelic imbalances of KCNQ1-FinA and KCNQ1-FinB specific cardiomyocyte.

Standard curve formed by KCNQ1-FinA specific plasmid mixes was used for determining allelic expression variation of KCNQ1-FinA specific cardiomyocytes (figure 8). Two different cardiac cell lines UTA.02201.LQT1 and UTA.00208.LQT1 contained mutation of interest were used for determination. The equation defined for standard curve ($y = 0{,}3528x + 2{,}4867$, where $y = \log_2$(WT/MUT) and $x = \Delta$Ct) was used to calculate $\log_2$(WT/MUT) values for specific cardiomyocyte samples by using their mean ΔCt values (n =3) counted from qPCR measured Ct values. For UTA.02201.LQT1-derived cardiomyocytes the calculated $\log_2$(WT/MUT) values was 1,475, indicating that they have location between 2:1 and 4:1 (WT:MUT) plasmid mixes on the standard curve (figure 8.). By using the same standard curve equation, $\log_2$(WT/MUT) value was defined to be 1,577 for UTA.00208.LQT1-derived cardiomyocytes. Therefore, they have also location between 2:1 and 4:1 plasmid mixes on the standard curve, but slightly closer to 4:1 plasmid mix than UTA.02201.LQT1 cardiomyocytes (figure 8.). Due to that defined $\log_2$(WT/MUT) values for both cardiomyocyte samples ranged approximately 0,5 between $\log_2$(WT/MUT) values of 2:1 and 4:1 plasmid mixed, it was decided to determine theoretical $\log_2$(WT/MUT) value for 3:1 plasmid mix that resulted in 1,58. By comparing $\log_2$(WT/MUT) values of cardiomyocyte samples with $\log_2$(WT/MUT)

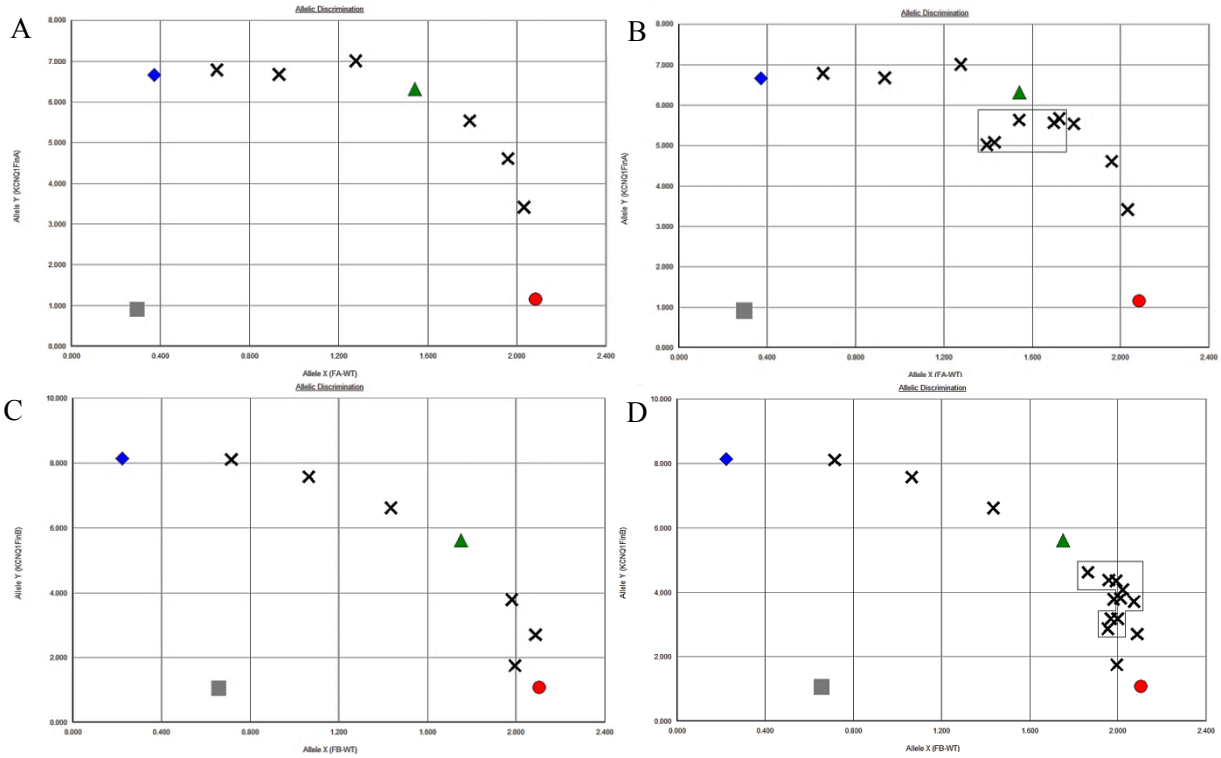

Figure 7. Allelic discrimination plots formed during allelic imbalance analyses of KCNQ1-FinA and KCNQ1-FinB specific cardiomyocytes. Red circles represent plasmid mixes contained only WT plasmid (1:0), while plasmid mixes contained only MUT plasmids (0:1) are described by blue diamonds. Green triangles symbolize plasmid mixes 1:1, in which allelic content of WT and MUT alleles is equal. Other plasmid mixes are represented by black crosses in order to avoid mixing with differently symbolized plasmid mixes. Non-template control is marked by grey square. All plasmid mixes and cardiomyocyte samples were analyzed as triplicates but in the figures one replicate from each sample is represented for clarity. (A) Allelic discrimination plot of KCNQ1-FinA specific plasmid mixes. (B) KCNQ1-FinA specific cardiomyocytes are located among plasmid mixes. The samples are separated from plasmid mixes with black boundaries in order to prevent mixing with plasmid mix samples having same symbols. (C) Allelic discrimination plot of KCNQ1-FinB specific plasmid mixes. (D) Locations of KCNQ1-FinB specific cardiomyocyte samples among plasmid mixes are separated with boundaries.

value of 3:1 plasmid ratio, it was observed relatively small differences in the defined values. Thus, according to these results allele-specific expression variation is occurring within both analyzed KCNQ1-FinA mutated cardiomyocytes (UTA.02201.LQT1 and UTA.00208.LQT1) and the allelic expression ratios are 3:1, indicating that wild type allele is expressed 3-fold as compared to mutant allele expression.

The allelic imbalance determination of KCNQ1-FinB specific cardiomyocytes were examined from standard curve made by KCNQ1-FinB specific plasmid mixes (figure 8.). As described

above in KCNQ1-FinA determination, the standard curve equation (y = 0,2048x + 1,6727) was used to define log_2(WT/MUT) values for KCNQ1-FinB specific cardiomyocyte samples generated from UTA.00118.LQT1 cell line. Four distinct cell samples were generated from the same cell line, and observed allelic imbalance results between them were convergent. In this section, results from two samples are represented in details in the figure 8. The calculated log_2(WT/MUT) values for those cardiomyocyte samples were 1,484 and 1,376, indicating that they located between 2:1 and 4:1 (WT:MUT) plasmid mixes, slightly closer to 2:1 plasmid mix, on the standard curve (figure 8.). When their log_2(WT/MUT) values were compared with theoretical 3:1 plasmid mix (1,58), smaller differences were observed between them, as was also occurred in the allelic imbalance determination of KCNQ1-FinA. Therefore, the detected allelic expression variation in these KCNQ1-FinB specific cardiomyocytes (UTA.00118.LQT1) results in three-fold expression of wild type allele as compared to mutant allele expression.

5.2.2. HERG-FinA and HERG-FinB mutations

Allelic expression variation of HERG-FinA and HERG-FinB specific cardiomyocytes were evaluated similarly as described above in the allelic imbalance determination of *KCNQ1* mutations. Mutation specific cDNA samples for HERG-FinA determination were generated from LQT2-specific cell lines UTA.03412.LQT2 and UTA.03810.LQT2. Thus, two different HERG-FinA specific cardiac cell lines derived from iPSCs of two mutation carriers were used for determination. LQT2-specific cardiac cell line used to evaluate allelic imbalance of HERG-FinB specific cardiomyocytes was UTA.00525.LQT2.

Allelic discrimination plots of plasmid mixes of both HERG mutations formed curves according to their wild type and mutant allelic contents (figure 9A, 9C). Therefore, all LQTS-specific plasmid mixes prepared to this allelic imbalance study produced similar allelic discrimination results (figure 7A, 7C, 9A, 9C), indicating that their wild type and mutant insert proportions were desired and suitable for reliable formatting standard curves. As can be seen from the allelic discrimination plot containing plasmid mixes and HERG-FinA specific cDNA samples (figure 9B), the clustering of cDNA samples among curve made by plasmid mixes differ from observed clustering of KCNQ1-FinA and KCNQ1-FinB specific samples on their allelic discrimination plots (figure 7B, 7D). The HERG-FinA cDNA samples (generated from UTA.03412.LQT2 and UTA.03810.LQT2 cell lines) clustered between 1:1

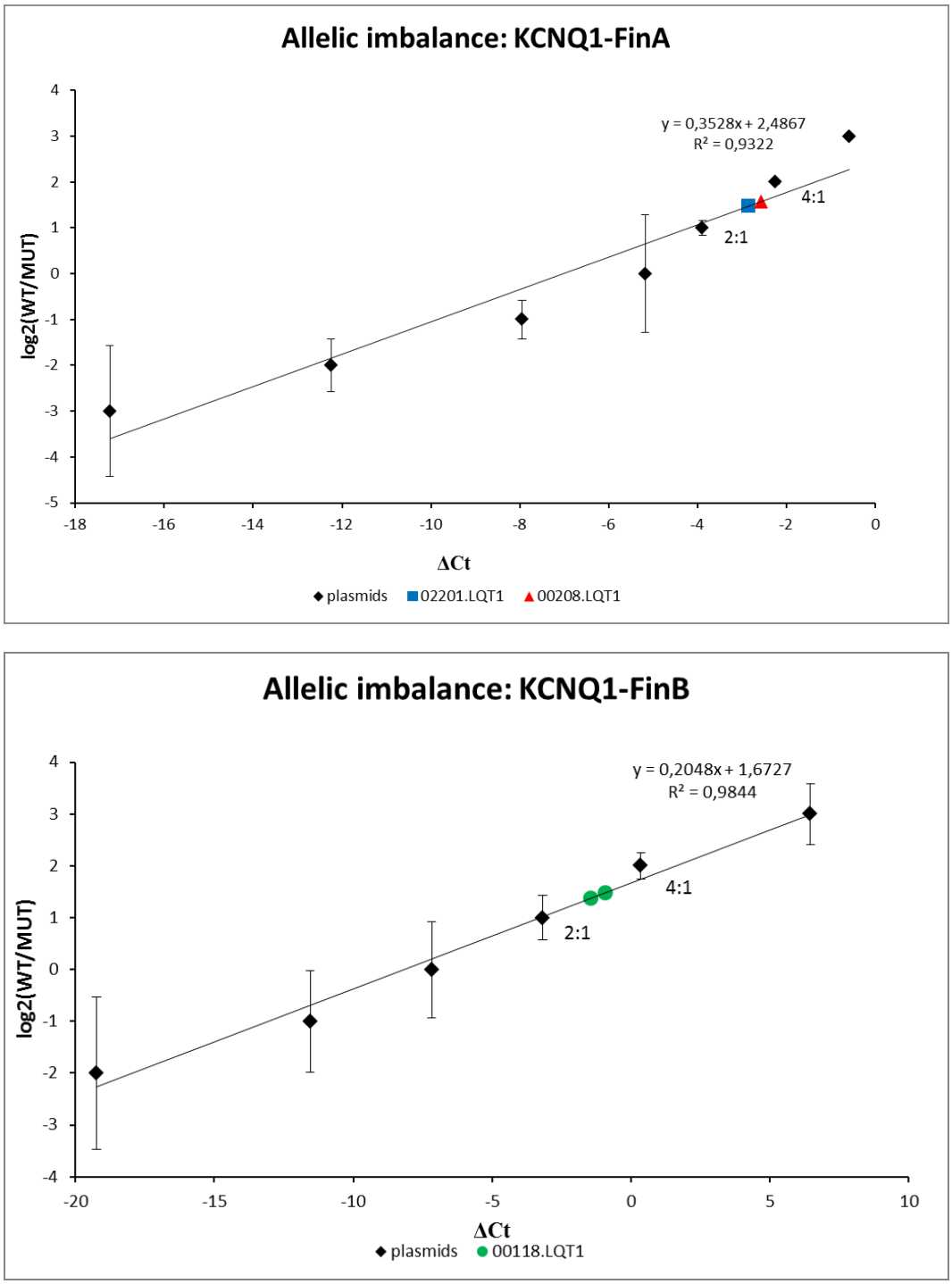

Figure 8. Allelic imbalance determinations of KCNQ1-FinA and KCNQ1-FinB specific cardiomyocytes by using plasmid-derived standard curve method. Plasmid mixes (8:1, 4:1, 2:1, 1:1, 1:2, 1:4, and 1:8) are symbolized with black diamonds in the figures. In KCNQ1-FinB standard curve, the 1:8 plasmid mix was not involved in standard curve formation due to the undetected fluorescence signals of VIC fluorophore. The ΔCt values for plasmid mixes are represented in statistical form of mean ± standard deviation (n=3). Allelic imbalance of KCNQ1-FinA specific cardiomyocytes was determined from two cardiac cells lines: UTA.00208.LQT1 marked by red triangle and UTA.02201.LQT1 marked by blue square on the standard curve. One KCNQ1-FinB specific cell line UTA.00118.LQT1 was used to determine allelic expression variation. Two UTA.00118.LQT1 samples are represented with green cycles on the standard curve.

and 1:2 (WT:MUT) plasmid mixes, indicating that allelic expression variation may be different within HERG-FinA mutated cardiomyocytes as compared to cardiomyocytes with specific *KCNQ1* mutations. The allelic discrimination plot of HERG-FinB specific determination (figure 9D) revealed that all analyzed samples, including control and HERG-FinB specific cardiac cell samples, were clustered around non-template control (NTC) samples. This was observed to occur in three different qPCR analyses by using re-transcribed HERG-FinB cDNA samples (generated from UTA.00525.LQT2) and control samples which amplification had been verified in earlier allelic imbalance determinations with qPCR system (data not shown). For this reason, allele-specific expression analysis could not perform for HERG-FinB specific cardiomyocytes.

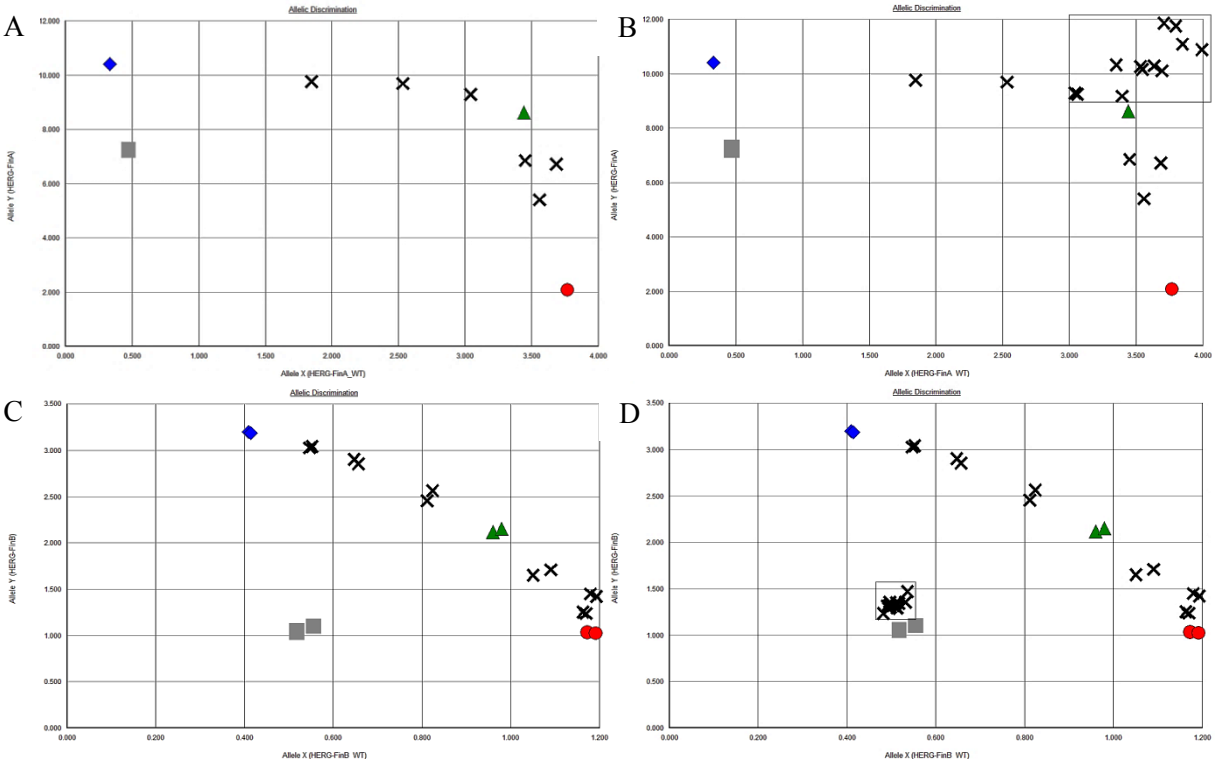

Figure 9. Allelic discrimination plots of HERG-FinA and HERG-FinB mutations. Used symbols are similar with the allelic discrimination plots of KCNQ1 mutations described in the previous section. (A) Allelic discrimination plot of HERG-FinA specific plasmid mixes. (B) Heterozygote HERG-FinA specific cardiomyocytes locate among plasmid mixes. (C) Allelic discrimination plot of HERG-FinB specific plasmid mixes. Two replicates are represented in the figure. (D) Locations of HERG-FinB specific cardiomyocyte samples and control samples on the allelic discrimination plot are beside with non-template control samples.

Standard curve formed by HERG-FinA specific plasmid mixes was used for determining allelic expression variation of HERG-FinA specific cardiomyocytes (figure 10.). Standard

curve equation (y = 0,6034x + 1,0161) was used to define locations of HERG-FinA cDNA samples on the standard curve. The calculated $\log_2$(WT/MUT) values for UTA.03412.LQT2 and UTA.03810.LQT2 samples were -0,2579 and -0,3878, respectively, resulted in locations between 1:1 and 1:2 (WT:MUT) plasmid mixes. According to these values, it was suggested that mutant samples locate closer with 1:1 plasmid mixes on the standard curve, but ΔCt values defined for them were closer with mean ΔCt value defined for 1:2 plasmid mix. Therefore, they locate in vicinity with 1:2 plasmid mix in the figure 10. The plasmid-derived standard curve revealed that allele-specific expression is also occurring within HERG-FinA specific cardiomyocytes, but it differ significantly from the allelic imbalances observed for KCNQ1-FinA and KCNQ1-FinB specific cardiomyocytes. According to this allelic imbalance determination, mutant allele can be expressed slightly higher than wild type allele within HERG-FinA specific cardiomyocytes, but the allelic expression difference is not remarkable.

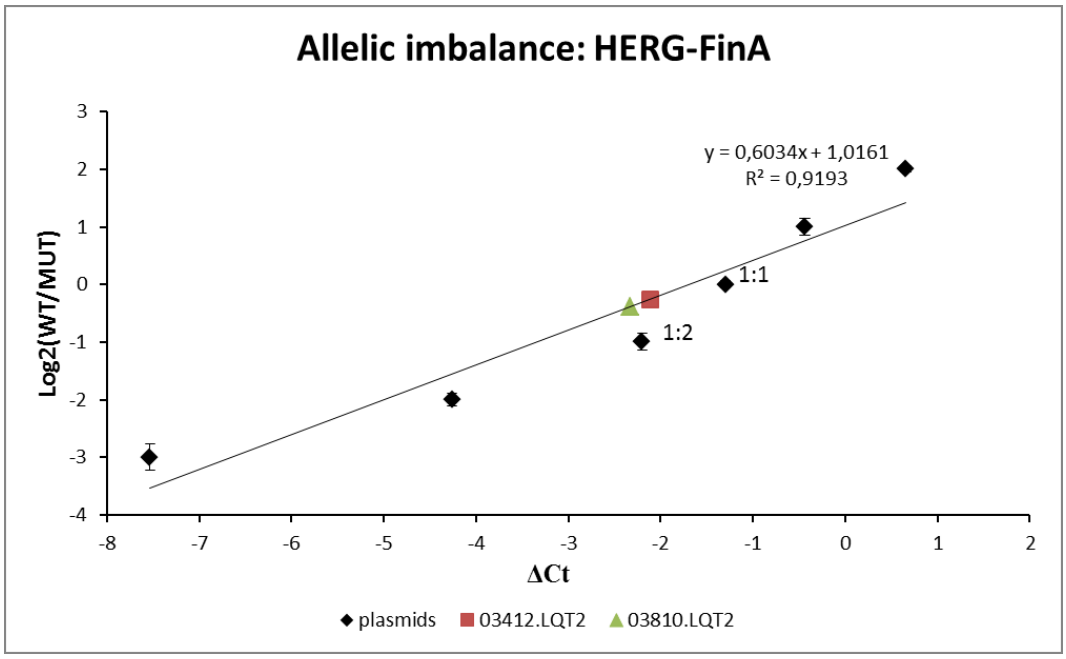

Figure 10. Allelic imbalance of HERG-FinA specific cardiomyocytes. The allelic imbalance of two different HERG-FinA specific cell samples from 03412.LQT2 (light red square) and 03810.LQT2 (light green triangle) cell lines were determined by using HERG-FinA specific standard curve. Locations of HERG-FinA samples were calculated from the equation of standard curve by using ΔCt values determined from amplification data.

5.3. Single-cell gene expression experiment

The amplification plot for low cell number sample (UTA.00208.LQT1) (figure 11A) revealed that detection ability of Single cell-to-CT™ Kit (Ambion®, Life Technologies Ltd.) was not sufficient to detect amplification of TNNT2, although the pre-amplification was performed

before qPCR analysis and the selected target TNNT2 is abundantly expressed in functional, beating cardiomyocytes. The amplification of endogenous reference, RPLP0 was, however, detected during qPCR analysis (figure 11A) but the amplification initiated in the late PCR cycles, approximately during PCR cycle 32 within UTA.00208.LQT1 samples. It indicates that the amount of RPLP0 template have been low. Amplifications of both targets, TNNT2 and RPLP0, were detected to occur within control samples (UTA.04311.WTs), as can be observed from their amplification plots (figure 11B, 11C). Although both targets were amplified in these control samples containing multiple cardiomyocytes the amplifications of TNNT2 were relatively poor, detected to initiate during PCR cycles 28 and 35; whereas RPLP0 amplification initiated during PCR cycles 21 and 27. According to these results, it suggested that some technical factors related to the used method might cause observed amplification differences between low cell number sample (UTA.00208.LQT1) and multiple cell samples (UTA.04311.WTs) leading to undetected and reduced TNNT2 amplifications, respectively.

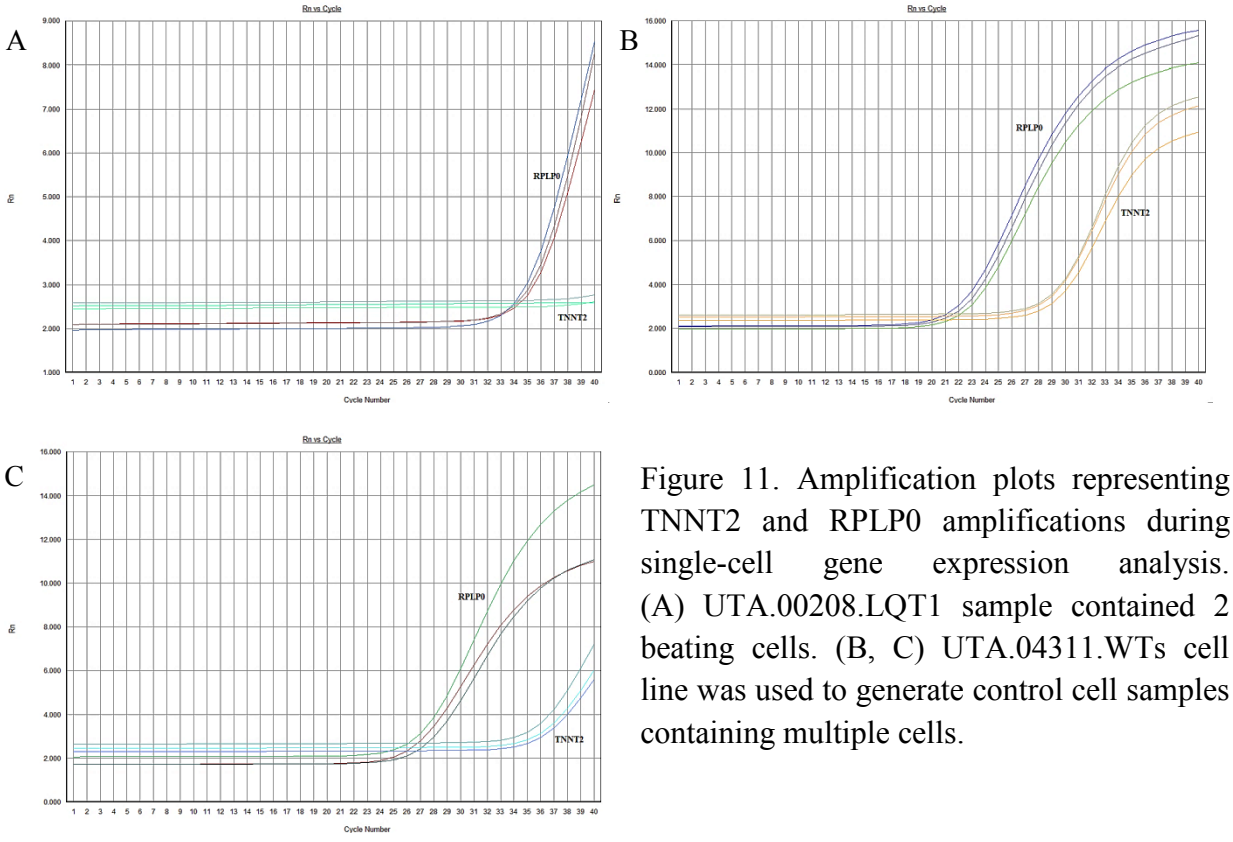

Figure 11. Amplification plots representing TNNT2 and RPLP0 amplifications during single-cell gene expression analysis. (A) UTA.00208.LQT1 sample contained 2 beating cells. (B, C) UTA.04311.WTs cell line was used to generate control cell samples containing multiple cells.

6. Discussion

This study demonstrated the capacity of quantitative real-time PCR to characterize specific gene expression features within iPSC-derived LQTS-specific cardiomyocytes. Three different experiments were performed using qPCR for analyzing either amplification of desired target genes or their allelic expression differences. The cells that were used in these experiments were heterozygous LQTS-specific cardiomyocytes containing four founder mutations in order to evaluate disease features occurring among Finnish population. All cardiomyocytes were differentiated from patient-specific induced pluripotent stem cells and their functionalities were characterized by evaluating expression of cardiac specific markers, such as cardiac troponin T2, α-actinin, myosin heavy chain and connexin-43, and electrophysiological features, including delayed repolarization phase and reduced K^+ ion currents, with MEA and patch clamp technology (Lahti et al., 2012). In addition, the control cardiomyocytes were generated from iPSCs of healthy individuals and their functionalities were verified similarly than was done for disease-specific cardiomyocytes.

6.1. Cell line characterization by using cell lysis -based method

In general, cell line characterization is performed by extracting total DNA or transcribing cDNA from isolated RNA of cell lines to be genotyped. However, nowadays many methods for cell characterization allow use of cell lysate directly for qPCR analysis with appropriate markers to perform amplification and detection of desired gene targets (Fox et al., 2012). Lysis release total DNA contents of lysed cell samples to be available for PCR amplification and therefore, it reduces the lack of DNA target templates that has been related to DNA extraction methods. In addition, cell lysis procedure facilitates and makes characterization faster due to that previously required DNA extractions are not necessitated before gene expression analysis with qPCR. Furthermore, the risk of potential contaminations and failures could occur during DNA extraction or cDNA transcription decrease. Especially cell lysis techniques are useful when gene expression profiles of low-sized or single cell samples are evaluated (Bengtsson et al., 2008).

Using TaqMan® Sample-to-SNP™ Kit (Applied Biosystems, Life Technologies Ltd.) to characterize LQT1-specific cardiac cell line contained KCNQ1-FinA mutation and two wild type cardiac cell lines, visible differences between LQT1-specific samples and WT samples were observed from their arrangements on the allelic discrimination plot caused by their

different allelic contents. According to the results of this experiment and results received from larger cell line characterization containing LQTS- and CPVT-specific lines (data not shown), cell lysis -based method was observed to be suitable for characterizing cardiac cell lines and its application can be expanded to characterize genetic contents of multiple cardiac disease-specific cell lines simultaneously in a routine manner. Non-lysed cellular components can disrupt qPCR analysis (Fox et al., 2012) but any disruption was not detected in these characterizations due to that analyzed sample sizes were relatively high, and therefore sufficient amount of target templates were present in PCR reactions although the cell lysis would not have been complete. Previously, there has been shown that TaqMan® Sample-to-SNP™ Kit (Applied Biosystems, Life Technologies Ltd.) have similar efficiency to detect specific SNPs than qPCR analysis performed from cell samples which DNAs has been isolated with conventional DNA extraction procedure (Nielsen et al., 2012), indicating that cell lysis -based methods are as accurate as conventional methods to detect specific genetic features within different cell types.

6.2. Allelic imbalance determinations of LQTS founder mutations

High phenotypic variation has been associated with long QT syndrome and typically disease phenotype varies even among family members carrying the same LQTS-causing mutation (Fodstad et al., 2004). Furthermore, approximately 50 % of diagnosed LQTS patients are completely asymptomatic (Toivonen et al., 2008) or have experienced minor cardiac events, such as occasional palpitations (Lahti et al., 2012). Due to that significant phenotypic variation it has been suggested that some genetic or non-genetic factors cause the variation among LQTS patients (Piippo et al., 2001; Fodstad et al., 2004). Allele-specific expression variation caused by epigenetic modifications has been considered to be potential factor underlying variable phenotypes (Saenen and Vrints, 2008) because it have been confirmed that allelic expression variation within human genes is relatively common and affect development of human phenotypes (Lo et al., 2003; Buckland, 2004). In addition, it has been previously shown that allele-specific expression can promote disease development (Chen et al., 2008). To evaluate impact of allele-specific expression on variable LQTS-related phenotype, the plasmid-derived standard curve method was used to determine allelic imbalances of cardiomyocytes specific for four Finnish founder mutations. The allelic imbalance determinations revealed that KCNQ1-FinA and KCNQ1-FinB specific cardiomyocytes expressed normal *KCNQ1* alleles with higher magnitude than corresponding mutant alleles leading to observed allelic proportions 3:1 (WT:MUT) in both cases. This

indicated that expressions of wild type alleles are three-fold higher than the expressions of mutated alleles within these LQT1-specific cardiomyocytes (UTA.02201.LQT1, UTA.00208.LQT1 and UTA.00118.LQT1).

The observed allelic imbalances for *KCNQ1* mutations differed from the previous allelic imbalance study performed using LQT1-specific cardiomyocytes contained heterozygous KCNQ1 mutation, R190Q (Moretti et al., 2010) in which equal expressions of wild type and R190Q-mutated alleles (1:1) were observed by using similar plasmid-derived standard curve method that has been used in this study. The R190Q mutation locates in cytoplasmic loop between transmembrane S2 and S3 segments (Moretti et al., 2010), whereas in contrast, KCNQ1-FinA (G589D) and KCNQ1-FinB (IVS7-2A>G) have locations in intracellular C-terminal end of the α-subunit (Fodstad et al., 2004). These both regions are related to highly pathogenic mutations due to that their defects affect significantly to channel functions (Giudicessi and Ackerman, 2012). The mechanisms identified from R190Q and G589D mutations are affect dominant negatively for protein trafficking (Moretti et al., 2010) and subunit assembly ability (Piippo et al., 2001), respectively. KCNQ1-FinB causes larger structural defect to α-subunit due to amino acid insertion that lead to complete loss of channel function (Fodstad et al., 2006). Thus, these *KCNQ1* mutations impair critically α-subunits' functions that result in reduction of I_{Ks} current through KCNQ1 channels, but their effects on current amplitude have been shown to be different. Moretti et al. (2010) observed that the I_{Ks} current reduced approximately 75 % in R190Q-mutated cardiomyocytes when were compared with control cardiomyocytes. As it have previously suggested that dominant negative effect of LQTS-causing mutations may cause more than 50 % reduction of the affected ion current, although wild type and mutant alleles are expressed equally within cells (Bezzina and Wilde, 2007). The observed reductions of I_{Ks} currents in KCNQ1-FinA specific (Saucermann et al., 2004) and KCNQ1-FinB specific (Fodstad et al., 2006) cardiomyocytes have been about 50 % and 28 %, respectively. The reduction of I_{Ks} current in KCNQ1-FinB specific cardiomyocytes (Fodstad et al., 2006) is consistent with the allelic imbalance results observed in this study for KCNQ1-FinB specific cardiomyocytes. However, it can be suggested that allelic ratio 3:1 occurred also within KCNQ1-FinA specific cardiomyocytes would produce less than 50 % current reduction that is usually related to equal allelic expression. Ion current reduction is, however, cell line -specific variable due to that cardiac cell lines are generated from patient-specific cells having their unique phenotypic features. Therefore, these measured I_{Ks} current

reductions (Saucermann et al., 2004; Fodstad et al., 2006) do not represent reliable the reductions occurring within cell lines used in this study (UTA.00208.LQT1, UTA.02201.LQT1 and UTA.00118.LQT1) although they contained same mutations.

On the other hand, it has been suggested that milder phenotypic effects of founder mutations within Finnish population have allowed their enrichment (Piippo et al., 2001). This allele-specific expression determination may support the fact that higher expression of wild type allele and suppressed expression of mutant allele can lead to milder phenotypic effects. In this study, used cardiomyocytes specific for KCNQ1-FinA and KCNQ1-FinB were generated from symptomatic patients who have prolonged QT intervals and experienced cardiac symptoms. In addition, patient-specific iPSC-derived cardiomyocytes have shown prolonged APDs and abnormal beating behaviors (Kiviaho et al., submitted). It is known that these both mutations are loss-of-function mutations and have dominant negative effects on channel function (Fodstad et al., 2004). Therefore, the detected allelic expression ratio 3:1 is suggested to cause suppressed expression of mutant allele resulting in production of higher amount of normal α-subunits which are able to form more functional repolarizing K^+ ion channels and thus phenotypic effects would be milder, such as increased I_{Ks} current amplitude and decreased arrhythmogenic susceptibility as compared with LQT1-specific cardiomyocytes containing rare mutations (Moretti et al., 2010). However, further investigations are required to confirm this hypothesis by using larger study populations containing cardiomyocytes specific for founder mutations and more rare LQT1-causing mutations which have similar effects to channel function. Therefore comparing allelic imbalances determined for founder mutations and rare mutations can reveal the potential of allelic expression variation to affect severities of disease phenotypes. Furthermore, this allelic imbalance method could be useful for evaluating impact of allele-specific expression on development of LQTS-related cardiac events by comparing cardiomyocytes derived from symptomatic and asymptomatic mutation carriers.

The allelic imbalance determination of HERG-FinA specific cardiomyocytes revealed that mutant alleles were slightly higher expressed than wild type alleles within used HERG-FinA specific cardiac cell lines (UTA.03412.LQT2 and UTA.03810.LQT2) but the expression variation between alleles was not thought to be significant. It was complicated to determine

allelic imbalance accurately due to that defined $\log_2$(WT/MUT) values were closer with $\log_2$(WT/MUT) value for 1:1 plasmid mix, while the defined ΔCt values were closer with ΔCt value for 1:2 plasmid mix (WT:MUT). Thus, the locations of specific cell samples were nearby 1:2 plasmid mix on the standard curve, although the allele-specific expressions were not supposed to be such variable due to $\log_2$(WT/MUT) values calculated from standard curve equation. The HERG-FinA mutation increases activation and deactivation rates of rapidly activating delayed rectifier K^+ ion channel and thereby reduce I_{Kr} current and delay repolarization (Piippo et al., 2000), indicating that it has significant effect on disease phenotype development. The used cDNA samples of HERG-FinA specific cardiomyocytes were generated from isolated RNAs of embryonic bodies and therefore other cell types presented in EBs might have disrupt detection and amplification of target HERG-FinA mutated alleles and corresponding wild type alleles within cardiomyocytes in qPCR analyses, leading to unspecific amplification of especially mutant allele. However, it can be possible that stochastic allelic expression variation (Elowitz et al., 2002) occurs within these HERG-FinA mutated cardiomyocytes and causes slightly overexpression of mutant alleles in a randomly manner. This study could not manage to show that HERG-FinA mutation may cause milder disease phenotype (Piippo et al., 2001) due to the observed allelic expression variation resulted in slightly higher mRNA levels of mutant α-subunits.

HERG-FinB specific allelic imbalance were not able to determined due to technical obstacles occurred during qPCR analyses that led to undetected amplification of HERG-FinB specific cardiomyocyte and control samples, although HERG-FinB specific plasmid mixes were amplified appropriately. It suggested that used TaqMan® Assay specific for HERG-FinB mutation did not work properly because control samples used in previous allelic imbalance determinations were amplified in those analyses as expected (data not shown) but they were not amplified in this determination and resulted in clustering close to non-template controls on the allelic discrimination plot. Possibly, reduced efficiency of HERG-FinB specific TaqMan® Assay causes decreased amplification and detection of target templates among various different templates included in cDNA samples, whereas detection of plasmid mixes is sufficient when disrupting distinct DNA templates are not presented in PCR reactions.

This allelic imbalance study detected only mRNA levels of wild type and mutant alleles and thus, observed allelic variations describe variations occurred between WT and mutant transcripts. According to measured mRNA transcripts for KCNQ1-FinA and KCNQ1-FinB specific cardiomyocytes, it suggested that 75 % of α-subunits are normal and 25 % are mutated α-subunits with defective function. Therefore, higher amount of functional channel-forming α-subunits are generated in these cardiomyocytes and adverse influences of dominant negative mutations reduce. In addition, when allele-specific expression is 3:1 (WT:MUT), the probability for K^+ ion channel consisting only wild type α-subunits is 32 % (Kiviaho et al., submitted), while the equal allelic expression produce probability of 6 % for channel containing only wild type α-subunits, as can be suggested to occur in HERG-FinA specific cardiomyocytes. However, translational processes and posttranslational modifications of proteins affect the final composition of WT and mutant α-subunits in cardiomyocytes and therefore, these mRNA-based allelic imbalance results are only estimations of potential proportions of α-subunits.

Allelic expression variation studies performed previously have observed that allele-specific expression is relatively common in many human genes (Lo et al., 2003). The cellular mechanisms causing gene expression variations are, however, highly unknown. It has been suggested that epigenetic modifications, such as hypermethylation of promoter regions or genetic alterations of non-coding regions may lead to higher expression of either allele (Buckland, 2004; Chen et al., 2008; Shen et al., 2011). The identified transcription start sites and promoter regions for *KCNQ1* and *KCNH2* genes (Luo et al., 2008) may enhance further studies to investigate epigenetic mechanisms underlying allele-specific expression revealed by this present allelic imbalance determinations. For example, high CpG island content of *KCNQ1* promoter region (Luo et al., 2008) enables evaluating effects of their potential methylation on observed allelic ratio 3:1 within KCNQ1-FinA and KCNC1-FinB specific cardiomyocytes.

Linear regression (R^2) values were defined for each formed plasmid-derived standard curve by using Microsoft Excel (2010) in order to estimate correlation between $\log_2$ value for plasmid ratio of wild type and mutant inserts (y-axis) and ΔCt values detected by qPCR system (x-axis). If standard curve's R^2 value is 1,0 the variables are completely correlating.

The defined R^2 values for KCNQ1-FinA, KCNQ1-FinB and HERG-FinA specific standard curves were 0,9322, 0,9844 and 0,9193, respectively. These observed nonlinearities might be caused by nonspecific hybridization of mutant probes of used TaqMan® Assays during PCR amplification phases in qPCR analyses. It can be observed from all allelic discrimination plot represented in this study, including cell line characterization and allelic imbalance experiments, that fluorescence signal intensities originated from FAM-labelled probes hybridized with mutant alleles (y-axis) are significantly higher as compared to fluorescence signal intensities from VIC-labelled probes bound with WT alleles (x-axis). The detected fluorescence intensity differences between mutant and wild type probes are approximately three-fold in the every allelic discrimination plot. Therefore, the mutant plasmids and mutant alleles within analyzed cDNA samples were detected with higher magnitudes than corresponding wild type fragments. In KCNQ1-FinA allelic imbalance determination (figure 8.) was observed that plasmid mixes containing higher or equal amount of WT plasmid than mutant plasmid (8:1, 4:1, 2:1, and 1:1) did not align linear with the plasmid mixes containing higher amount of mutant plasmid (1:2, 1:4, and 1:8), influencing directly for Ct values determined for wild type inserts during amplification and therefore calculating of ΔCt values used for standard curve formation. The nonspecific binding of mutant probes with wild type templates was tried to reduce by increasing annealing temperature from 60 °C to upwards but even one degree lifting to 61 °C impacted adversely on amplification of all plasmid mixes (data not shown). Thus, further allelic imbalance determinations were decided to perform at annealing temperature of 60 °C.

The linear regression of KCNQ1-FinB specific standard curve was slightly better (R^2 = 0,9844) than linear regressions of KCNQ1-FinA and HERG-FinA specific standard curves (R^2 = 0,9322 and R^2 = 0,9193, respectively) but still the R^2 value was not as good as the standard curve can be considered as linear. However, nonspecific hybridization of mutant probes occurred in KCNQ1-FinA and HERG-FinA specific analyses were more significant than occurred in KCNQ1-FinB specific analysis, reflecting better linear alignment of plasmid mixes on the standard curve. The nonspecific binding, however, led to undetected Ct values of WT plasmids in the 1:8 plasmid mixes and therefore the standard curve was generated using only the remaining plasmid ratios. The amplification data of HERG-FinA specific determination revealed that FAM fluorophore has produced fluorescent signals even within non-template controls and control cDNA samples, suggesting that mutant probes might have

degraded in used TaqMan® Assay leading to detected fluorescence signals from free FAM fluorophores rather than their nonspecific binding during the qPCR analysis. Due to this observation the allelic imbalance results of HERG-FinA specific cardiomyocytes are not reliable and thus, further studies are required for its evaluation.

6.3. Evaluating TNNT2 expression at low cell level

Cell populations are commonly heterogeneous resulting in different behavioral and functional features of individual cells among the population (Kalisky et al., 2011; Narsinh et al., 2011; Ståhlberg et al., 2011). For evaluating heterogeneity within cardiomyocyte population, Single cell-to-CT™ Kit (Ambion®, Life Technologies Ltd.) was used to quantify relative gene expression of cardiac troponin T2 (TNNT2) within cardiomyocyte samples contained two beating cells (UTA.00208.LQT1). The TNNT2 amplification was not detected from low-sized samples although amplification of housekeeping gene, RPLP0 occurred. Similar results were detected from cardiomyocyte sample containing seven beating cells (data not shown), indicating that the used method was not efficient to detect specific gene expression within defined 1-10 cell sample size. To evaluate reasons for the failed detection of abundantly expressed TNNT2, few potential causes were arisen. Pre-amplification was performed by using pooled TNNT2 and RPLP0 markers that might have led to competition between them during PCR amplification and production of higher amount of amplified RPLP0 than TNNT2 target (Peixoto et al., 2004). For this reason, the template amounts of TNNT2 may have been extremely low in qPCR analyses and therefore detection ability of qPCR system has not been sufficient to measure its amplification. For future single-cell gene expression studies, primer competition has to be evaluated before qPCR analyses (Ciriza et al., 2012). If any competition between used markers is observed, other housekeeping gene has to select to normalize expression of target gene. For example, PPIA could be an appropriate choice to be housekeeping gene for normalizing TNNT2 expression within cardiomyocytes due to that it has similar reaction efficiency than RPLP0 has (Kosloski et al., 2009). In addition, before qPCR analysis the pre-amplified samples were diluted 1:20 according to manufacturer's protocol that could have been too much for the low-sized samples leading to further reduction of template amount. In next time, single-cell gene expression analysis using Single cell-to-CT™ Kit (Ambion®, Life Technologies Ltd.) is preferred to perform with non-diluted or less diluted single cell samples in order to enhance detection efficiency of the method. However, TNNT2 amplifications were detected from control cardiomyocyte samples contained plenty of cells, which excluded the doubt about nonfunctional TaqMan® Assay of TNNT2. It was,

however, observed that amplifications were relatively low than could be assumed for abundantly expressed gene (Bengtsson et al., 2008). Therefore, results from controls were in consistent with observed fact that amount of TNNT2 template may have decreased during this single-cell gene expression analysis, resulting in higher amplifications of RPLP0 gene within all analyzed cardiomyocytes.

7. Conclusions

In conclusion, the quantitative real-time PCR is appropriate method for characterizing specific genetic features of LQTS-specific cardiomyocytes derived from patient-specific induced pluripotent stem cells. Cardiac cell lines can be characterized using cell lysis -based genotyping methods without any observed disruptions caused by non-lysed cellular components. Therefore, the method can be used for characterize distinct cardiac disease-specific cell lines effectively and accurately. In this study performed single-cell gene expression analysis was not succeeded and thus further studies are required before gene expression can be evaluated within a single cardiomyocyte.

Allelic imbalance determination by using plasmid-derived standard curve method revealed that allele-specific expression between wild type and mutant alleles is occurred with proportion 3:1 (WT:MUT) within KCNQ1-FinA and KCNQ1-FinB specific cardiomyocytes. Therefore, allelic expression variation may be a potential genetic factor affecting phenotypic variation related to long QT syndrome. The allelic imbalance occurring within LQT1-specific cardiomyocytes containing Finnish founder mutations can also elucidate the presumption that founder mutations may cause milder phenotypic effects permitted their enrichment among Finnish population. However, to confirm these hypotheses larger study populations are required that contain LQTS-specific cardiomyocytes generated from patients carrying Finnish founder mutations and more rare LQTS-associated mutations in order to verify impact of allelic imbalance on phenotypic variation and milder phenotypic effects. In addition, allelic expression variation's effect on phenotypic severity can be investigated with determinations based on cardiomyocytes generated from symptomatic and asymptomatic patients. Furthermore, the plasmid-derived standard curve method represented in this study enables to evaluate impacts of allelic expression variations on pathogenesis of other heterozygous cardiac disorder that inherent autosomal dominantly way, such as catecholaminergic polymorphic ventricular tachycardia (CPVT) and hypertrophic cardiomyopathy (HCM).

8. References

Abbott GW, Sesti F, Splawski I, Buck ME, Lehmann MH, Timothy KW, et al. MiRP1 Forms I_{Kr} Potassium Channels with HERG and Is Associated with Cardiac Arrhythmia. Cell. 1999; 97: 175 – 187.

Ackerman MJ. Genotype-phenotype relationships in congenital long QT syndrome. Journal of Electrocardiology. 2005; 38: 64 – 68.

Amin AS, Tan HL, Wilde AAM. Cardiac ion channels in health and disease. Heart Rhythm. 2010; 7: 117 – 126.

Arnaout R, Ferrer T, Huisken J, Spitzer K, Stainier DYR, Tristani-Firouzi M, et al. Zebrafish model for human long QT syndrome. PNAS. 2007; 104 (27): 11316 – 11321.

Arya M, Shergill IS, Williamson M, Gommersall L, Arya N, Patel HRH. Basic principles of real-time quantitative PCR. Expert Rev. Mol. Diagn. 2005; 5 (2): 209 – 219.

Bengtsson M, Hemberg M, Rorsman P, Ståhlberg A. Quantification of mRNA in single cells and modelling of RT-qPCR induced noise. BMC Molecular Biology. 2008; 9: 63.

Bezzina CR, Wilde AAM. Genetic Basis for Cardiac Arrhythmias. Cardiovascular Medicine. Third Edition. 2007; 2577 – 2598. Springer London. ISBN 978-1-84628-188-4

Brouzes E, Medkova M, Savenelli D, Marran D, Twardowski M, Hutchison JB, et al. Droplet microfluidic technology for single-cell high-throughput screening. PNAS. 2009; 106 (34): 14195 – 14200.

Buckland PR. Allele-specific gene expression differences in humans. Human Molecular Genetics. 2004; 13 (2): R255 – R260.

Chen L, Marquardt ML, Tester DJ, Sampson KJ, Ackerman MJ, Kass RS. Mutation of an A-kinase-anchoring protein causes long-QT syndrome. PNAS. 2007; 104 (52): 20990 – 20995.

Chen X, Weaver J, Bove BA, Vanderveer LA, Weil SC, Miron A, et al. Allelic imbalance in BRCA1 and BRCA2 gene expression is associated with an increased breast cancer risk. Human Molecular Genetics. 2008; 17 (9): 1336 – 1348.

Ciriza J, Hall D, Lu A, De Sena JR, Al-Kuhlani M, Garcia-Ojeda ME. Single-Cell Analysis of Murine Long-Term Hematopoietic Stem Cells Reveals Distinct Patterns of Gene Expression during Fetal Migration. PLoS ONE. 2012; 7 (1): e30542.

Clancy CE, Rudy Y. Cellular consequences of HERG mutations in the long QT syndrome: precursors to sudden cardiac death. Cardiovascular Research. 2001; 50: 301 – 313.

Egashira T, Yuasa S, Suzuki T, Aizawa Y, Yamakawa H, Matsuhashi T, et al. Disease characterization using LQTS-specific induced pluripotent stem cells. Cardiovascular Research. 2012; 95: 419 – 429.

Elowitz MB, Levine AJ, Siggia ED, Swain PS. Stochastic Gene Expression in a Single Cell. Science. 2002; 297: 1183 – 1186.

Fodstad H, Bendahhou S, Rougier J-S, Laitinen-Forsblom PJ, Barhanin J, Abriel H, et al. Molecular characterization of two founder mutations causing long QT syndrome and identification of compound heterozygous patients. Ann Med. 2006; 38: 294 – 304.

Fodstad H, Swan H, Laitinen P, Piippo K, Paavonen K, Viitasalo M, et al. Four potassium mutations account for 73% of the genetic spectrum underlying long-QT syndrome (LQTS) and provide evidence for a strong founder effect in Finland. Ann Med. 2004; 36 (Suppl 1): 53 – 63.

Fox BC, Devonshire AS, Baradez M-O, Marshall D, Foy CA. Comparison of reverse transcription-quantitative polymerase chain reaction methods and platforms for single cell gene expression analysis. Analytical Biochemistry. 2012; 427: 178 – 186.

Freeman TC, Lee K, Richardson PJ. Analysis of gene expression in single cells. Current Opinion in Biotechnology. 1999; 10: 579 – 582.

Giudicessi JR, Ackerman MJ. Potassium-channel mutations and cardiac arrhythmias– diagnosis and therapy. Nat. Rev. Cardiol. 2012; 9: 319 – 332.

Glotzbach JP, Januszyk M, Vial IN, Wong VW, Gelbard A, Kalisky T, et al. An Information Theoretic, Microfluidic-Based Single Cell Analysis Permits Identification of Subpopulations among Putatively Homogeneous Stem Cells. PLoS ONE. 2011; 6 (6): e21211.

Grant AO. Cardiac Ion Channels. Circ Arrhythmia Electrophysiol. 2009; 2: 185 – 194.

Heid CA, Stevens J, Livak KJ, Williams PM. Real Time Quantitative PCR. Genome Research. 1996; 6: 986 – 994.

Inoue H, Yamanaka S. The Use of Induced Pluripotent Stem Cells in Drug Development. Clinical Pharmacology & Therapeutics. 2011; 89 (5): 655 – 661.

Itzhaki I, Maizels L, Huber I, Zwi-Dantsis L, Caspi O, Winterstern A, et al. Modelling the long QT syndrome with induced pluripotent stem cells. Nature. 2011; 471: 225 – 229.

Jespersen T, Grunnet M, Olesen S-P. The KCNQ1 Potassium Channel: From Gene to Physiological Function. Physiology. 2005; 20: 408 – 416.

Kalisky T, Blainey P, Quake SR. Genomic Analysis at the Single-Cell Level. Annu Rev Genet. 2011; 45: 431 – 445.

Kim K, Doi A, Wen B, Ng K, Zhao R, Cahan P, et al. Epigenetic memory in induced pluripotent stem cells. Nature. 2010; 467 (7313): 285 – 290.

Kiviaho AL, Ahola A, Larsson K, Kujala K, Pekkanen-Mattila M, Venäläinen H, et al. Long QT syndrome type 1 -specific cardiomyocytes carrying different mutations reveal distinct electrophysiological and mechanical phenotypes. Submitted.

Kontula K. Supisuomalaiset sydäntautigeenit. Duodecim. 2005; 121: 2665 – 79.

Kosloski LM, Bales IK, Allen KB, Walker BL, Borkon AM, Stuart RS, et al. Purification of cardiac myocytes from human heart biopsies for gene expression analysis. Am J Physiol Heart Circ Physiol. 2009; 297: H1163 – H1169.

Laflamme MA, Chen KY, Naumova AV, Muskheli V, Fugate JA, Dupras SK, et al. Cardiomyocytes derived from human embryonic stem cells in pro-survival factors enhance function of infarcted rat hearts. Nat. Biotechnol. 2007; 25 (9): 1015 – 1024.

Lahti AL, Kujala VJ, Chapman H, Koivisto A-P, Pekkanen-Mattila M, Kerkelä E, et al. Model for long QT syndrome type 2 using human iPS cells demonstrates arrhythmogenic characteristics in cell culture. Disease Models & Mechanisms. 2012; 5: 220 – 230.

Laitinen P, Fodstad H, Piippo K, Swan H, Toivonen L, Viitasalo M, et al. Survey of the Coding Region of the HERG Gene in Long QT Syndrome Reveals Six Novel Mutations and an Amino Acid Polymorphism with Possible Phenotypic Effects. Hum Mutant. 2000; 15: 580 – 581.

Livak KJ, Schmittgen TD. Analysis of Relative Gene Expression Data Using Real-Time Quantitative PCR and the $2^{-\Delta\Delta C}{}_T$ Method. Methods. 2001; 25: 402 – 408.

Lo HS, Wang Z, Hu Y, Yang HH, Gere S, Buetow KH, et al. Allelic Variation in Gene Expression Is Common in the Human Genome. Genome Res. 2003; 13: 1855 – 1862.

Luo X, Xiao J, Lin H, Lu Y, Yang B, Wang Z. Genomic structure, transcriptional control, and tissue distribution of HERG1 and KCNQ1 genes. Am J Physiol Heart Circ Physiol. 2008; 294: H1371 – H1380.

Marjamaa A, Salomaa V, Newton-Chen C, Porthan K, Reunanen A, Karanko H, et al. High prevalence of four long QT syndrome founder mutations in the Finnish population. Ann Med. 2009; 41: 234 – 240.

Matsa E, Rajamohan D, Dick E, Young L, Mellor I, Staniforth A, et al. Drug evaluation in cardiomyocytes derived from human induced pluripotent stem cells carrying a long QT syndrome type 2 mutation. European Heart Journal. 2011; 32: 952 – 962.

Medeiros-Domingo A, Kaku T, Tester DJ, Iturralde-Torres P, Itty A, Ye B, et al. SCN4B-Encoded Sodium Channel β4 Subunit in Congenital Long-QT Syndrome. Circulation. 2007; 116: 134 – 142.

Mohler PJ, Schott J-J, Gramolini AO, Dilly KW, Guatimosim S, duBell WH, et al. Ankyrin-B mutation causes type 4 long-QT cardiac arrhythmia and sudden cardiac death. Nature. 2003; 421 (6923): 634 – 639.

Moretti A, Bellin M, Welling A, Jung CB, Lam JT, Bott-Flugel L, et al. Patient-Specific Induced Pluripotent Stem-Cell Models for Long-QT Syndrome. N Engl J Med. 2010; 363 (15): 1397 – 1409.

Moretti A, Laugwitz K-L, Dorn T, Sinnecker D, Mummery C. Pluripotent Stem Cell Models of Human Heart Disease. Cold Spring Harb Perspect Med. 2013; 3: a014027.

Moss AJ, Shimizu W, Wilde AAM, Towbin JA, Zareba W, Robinson JL, et al. Clinical Aspects of Type-1 Long-QT Syndrome by Location, Coding Type, and Biophysical Function of Mutations Involving the KCNQ1 Gene. Circulation. 2007; 115 (19): 2481 – 2489.

Mummery C, Ward-van Oostwaard D, Doevendans P, Spijker R, van den Brink S, Hassink R, et al. Differentiation of Human Embryonic Stem Cells to Cardiomyocytes: Role of Coculture with Visceral Endoderm-Like Cells. Circulation. 2003; 107: 2733 – 2740.

Mummery CL, Zhang J, Ng ES, Elliott DA, Elefancy AG, Kamp TJ. Differentiation of Human Embryonic Stem Cells and Induced Pluripotent Stem Cells to Cardiomyocytes: A Methods Overview. Circ Res. 2012; 111: 344 – 358.

Narsinh KH, Sun N, Sanchez-Freire V, Lee AS, Almeida P, Hu S, et al. Single cell transcriptional profiling reveals heterogeneity of human induced pluripotent stem cells. J Clin Invest. 2011; 121 (3): 1217 – 1221.

Neyroud N, Tesson F, Denjoy I, Leibovici M, Donger C, Barhanin J, et al. A novel mutation in the potassium channel gene KVLQT1 causes the Jervell and Lange-Nielsen cardioauditory syndrome. Nature Genetics. 1997; 15: 186 – 189.

Nielsen PB, Petersen MS, Ystaas V, Andersen RV, Hansen KM, Blaabjerg V, et al. Sample-to-SNP kit: A reliable, easy and fast tool for the detection of HFE p.H63D and p.C282Y variations associated to hereditary hemochromatosis. Gene. 2012; 507: 79 – 84.

Peixoto A, Monteiro M, Rocha B, Veiga-Fernandes H. Quantification of Multiple Gene Expression in Individual Cells. Genome Research. 2004; 14: 1938 – 1947.

Pekkanen-Mattila M, Kerkelä E, Tanskanen JMA, Pietilä M, Pelto-Huikko M, Hyttinen J, et al. Substantial variation in the cardiac differentiation of human embryonic stem cell lines derived and propagated under the same conditions – a comparison of multiple cell lines. Ann Med. 2009; 41: 360 – 370.

Piippo K, Laitinen P, Swan H, Toivonen L, Viitasalo M, Pasternack M, et al. Homozygosity for a HERG Potassium Channel Mutation Causes a Severe Form of Long QT Syndrome: Identification of an Apparent Founder Mutation in the Finns. J Am Coll Cardiol. 2000; 35 (7): 1919 – 1925.

Piippo K, Swan H, Pasternack M, Chapman H, Paavonen K, Viitasalo M, et al. A Founder Mutation of the Potassium Channel KCNQ1 in Long QT Syndrome: Implications for Estimation of Disease Prevalence and Molecular Diagnostics. J Am Coll Cardiol. 2001; 37 (2): 562 – 568.

Raj A, Rifkin SA, Andersen E, van Oudenaarden A. Variability in gene expression underlies incomplete penetrance. Nature. 2010; 463: 913 – 918.

Roden DM, Balser JR, George AL, Anderson ME. Cardiac Ion Channels. Annu. Rev. Physiol. 2002; 64: 431 – 475.

Roden DM. Long-QT Syndrome. N Engl J Med. 2008; 358: 169 – 176.

Saenen JB, Vrints CJ. Molecular aspects of the congenital and acquired Long QT Syndrome: Clinical implications. Journal of Molecular and Cellular Cardiology. 2008; 44: 633 – 646.

Salama G, London B. Mouse models of long QT syndrome. J Physiol. 2007; 578.1: 43 – 53.

Sanguinetti MC, Tristani-Firouzi M. hERG potassium channels and cardiac arrhythmia. Nature. 2006; 440: 463 – 469.

Saucermann JJ, Healy SN, Belik ME, Puglisi JL, McCulloch AD. Proarrhythmic Consequences of a KCNQ1 AKAP-Binding Domain Mutation: Computational Models of Whole Cells and Heterogeneous Tissue. Circ Res. 2004; 95: 1216 – 1224.

Schmitt N, Schwarz M, Peretz A, Abitbol I, Attali B, Pongs O. A recessive C-terminal Jervell and Lange-Nielsen mutation of the KCNQ1 channel impairs subunit assembly. EMBO J. 2000; 19 (3): 332 – 340.

Schulze-Bahr E, Wang Q, Wedekind H, Haverkamp W, Chen Q, Sun Y, et al. KCNE1 mutations cause Jervell and Lange-Nielsen syndrome. Nature Genetics. 1997; 17: 267 – 268.

Shen J, Medico L, Zhao H. Allelic imbalance in BRCA1 and BRCA2 Gene Expression and Familial Ovarian Cancer. Cancer Epidemiol Biomarkers Prev. 2011; 20 (1): 50 – 56.

Splawski I, Shen J, Timothy KW, Lehmann MH, Priori S, Robinson JL, et al. Spectrum of Mutations in Long-QT Syndrome Genes: KVLQT1, HERG, SCN5A, KCNE1, and KCNE2. Circulation. 2000; 102: 1178 – 1185.

Splawski I, Timothy KW, Sharpe LM, Decher N, Kumar P, Bloise R, et al. $Ca_V1.2$ Calcium Channel Dysfunction Causes a Multisystem Disorder Including Arrhythmia and Autism. Cell. 2004; 119 (1): 19 – 31.

Splawski I, Timothy KW, Vincent GM, Atkinson DL, Keating MT. Molecular basis of the long-QT syndrome associated with deafness. N Engl J Med. 1997; 336 (22): 1562 – 1567.

Splawski I, Tristani-Firouzi M, Lehmann MH, Sanguinetti MC, Keating MT. Mutations in the hminK gene cause long QT syndrome and suppress I_{Ks} function. Nature Genetics. 1997; 17 (3): 338 – 340.

Ståhlberg A, Kubista M, Åman P. Single-cell gene-expression profiling and its potential diagnostic applications. Expert Rev. Mol. Diagn. 2011; 11 (7): 735 – 740.

Takahashi K, Tanabe K, Ohnuki M, Narita M, Ichisaka T, Tomoda K, et al. Induction of Pluripotent Stem Cells from Adult Human Fibroblasts by Defined Factors. Cell. 2007; 131: 861 – 872.

Takahashi K, Yamanaka S. Induction of Pluripotent Stem Cells from Mouse Embryonic and Adult Fibroblast Cultures by Defined Factors. Cell. 2006; 126: 663 – 676.

Taniguchi K, Kajiyama T, Kambara H. Quantitative analysis of gene expression in a single cell by qPCR. Nature Methods. 2009; 6 (7): 503 – 506.

Toivonen L, Swan H, Viitasalo M, Hartikainen J, Happonen J-M, Virtanen V, et al. Pitkä QT -oireyhtymä: kansallinen suositus. Duodecim. 2008: 124; 902 – 12.

Tristani-Firouzi M, Jensen JL, Donaldson MR, Sansone V, Meola G, Hahn A, et al. Functional and clinical characterization of KCNJ2 mutations associated with LQT7 (Andersen syndrome). J. Clin. Invest. 2002; 110 (3): 381 – 388.

Ueda K, Valdivia C, Medeiros-Domingo A, Tester DJ, Vatta M, Farrugia G, et al. Syntrophin mutation associated with long QT syndrome through activation of the nNOS-SCN5A macromolecular complex. PNAS. 2008; 105 (27): 9355 – 9630.

Vatta M, Ackerman MJ, Ye B, Makielski JC, Ughanze EE, Taylor EW, et al. Mutant Caveolin-3 Induces Persistent Late Sodium Current and Is Associated With Long-QT Syndrome. Circulation. 2006; 114: 2104 – 2112.

Vincent GM. The Molecular Genetics of the Long QT Syndrome: Genes Causing Fainting and Sudden Death. Annu. Rev. Med. 1998; 49: 263 – 274.

White AK, Vanlnberghe M, Petriv OI, Hamidi M, Sikorski D, Marra MA, et al. High-throughput microfluidic single-cell RT-qPCR. PNAS. 2011; 108 (34): 13999 – 14004.

Yoshida Y, Yamanaka S. iPS cells: A source of cardiac regeneration. Journal of Molecular and Cellular Cardiology. 2011; 50: 327 – 332.

Yu J, Vodyanik MA, Smuga-Otto K, Antosiewicz-Bourget J, Frane JL, Tian S, et al. Induced Pluripotent Stem Cell Lines Derived from Human Somatic Cells. Science. 2007; 318 (5858): 1917 – 1920.

Zhang J, Klos M, Wilson GF, Herman AM, Lian X, Raval KK, et al. Extracellular Matrix Promotes Highly Efficient Cardiac Differentiation of Human Pluripotent Stem Cells: The Matrix Sandwich Method. Circ Res. 2012; 111 (9): 1125 – 1136.

Zhang J, Wilson GF, Soerens AG, Koonce CH, Yu J, Palecek SP, et al. Functional Cardiomyocytes Derived from Human Induced Pluripotent Stem Cells. Circ Res. 2009; 104 (4): e30 – e41.

Zwi L, Caspi O, Arbel G, Huber I, Gepstein A, Park I-H, et al. Cardiomyocyte Differentiation of Human Induced Pluripotent Stem Cells. Circulation. 2009; 120: 1513 – 1523.